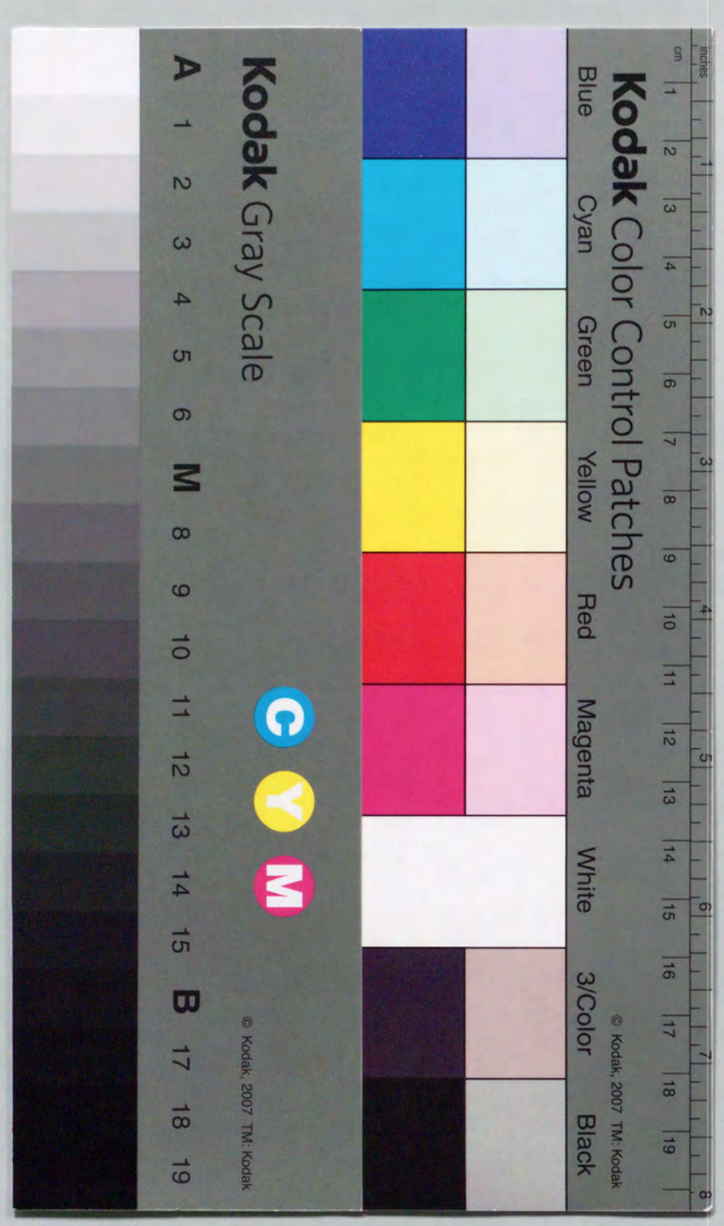

Green Function and Density Functional Approaches to Non Born-Oppenheimer and Proton and Electron Cooperative Systems

Yasuteru Shigeta

March, 2000

Department of Chemistry, Graduate School of Science,
Osaka University, Toyonaka 560-0043, Japan

Green Function and Density Functional Approaches to Non Born-Oppenheimer and Proton and Electron Cooperative Systems

Yasuteru Shigeta

March, 2000

Department of Chemistry, Graduate School of Science,
Osaka University, Toyonaka 560-0043, Japan

Acknowledgment

The present work has been completed under the supervision of Professor Kizashi Yamaguchi. The author would like to express sincere gratitude for many valuable discussions, suggestions and continued encouragement. The author is indebted to Professor Hidemi Nagao for collaboration, fruitful discussions, suggestions and encouragement throughout the course of the present study. He wishes to express his sincere gratitude to Professor Kiyoshi Nishikawa for helpful discussions, suggestions and encouragement throughout his research activity including the present study.

He wishes to thank to Dr. Koji Ohta, Dr. Kenji Kamada, Dr. Keiko Tawa, and Kenji Kiyohara for their helpful discussions about nonlinear optics both experimental and theoretical sides at Osaka National Research Institute. He wishes to thank to Dr. Kenji Kinugawa for fruitful discussions and collaboration with him. He also acknowledges Professor Masahiko Suhara, Professor Kazuo Endo, Dr. Masaharu Mizuno, Dr. Hiroyuki Kawabe, and all the members of the theoretical chemistry laboratory, Kanazawa university. He wishes to thank to Dr. Takashi Kawakami, Dr. Syusuke Yamanaka, Dr. Masaki Mitani, Dr. Hideaki Takahashi, Dr. Masayoshi Nakano, and Professor Yasunori Yoshioka for their continued encouragement and helpful discussions. He also thanks all the members of the quantum chemistry laboratory, graduate school of science, Osaka University.

He also is grateful to Professor Fredy Aryasetiawan, Dr. Masanori Tachikawa, Dr. Eric Shirley, Dr. Martin Springer, Dr. Bengt Holm, and Dr. Yuji Suwa for sending many manuscripts and doctoral thesis.

The author's works were supported by Research Fellowships of the Japan Society for the Promotion of Science for Young Scientist from January 1999 to March 2000.

Last, the author wishes to thank his parents for many years of encouragements and their affections.

Contents

Part I

Development of molecular theory without the Born- Oppenheimer approximation

Chapter 1

Introduction

The quantum mechanical behavior of molecules and molecular subunits in condensed matter, which is usually observed at low temperatures, is a subject of considerable current interests in experiments[1]-[14]. Substitution of hydrogen by deuterium leads to large isotope effects. For example, transition temperature from a ferroelectric phase to paraelectric phase of KH_2PO_4 crystal increases by 90 In such systems, coupling of the electronic structure with protonic motions is crucial for describing the transition properties. In general, the position of proton and deuteron can not be determined precisely by the X-ray diffraction experiments because of the weak scattering power of the hydrogen atom. Also quantum mechanical fluctuation makes the determination of the position of a proton more difficult at a more fundamental level. On the other hand, density of the proton and deuteron in crystals are obtained by the neutron diffraction experiments. Therefore, at least in crystalline systems, it may be preferable to describe the proton not as the point charge but as density distribution of a quantum mechanical particle. There are a few theoretical methods to determine the nuclear and electronic densities in molecules and bulk systems simultaneously.

One of the most fundamental approximations for the molecular and crystalline structure is the Born-Oppenheimer approximation (BOA) [15]. The basic idea of the BOA is to separate the degree of freedom of a molecule into the electronic, vibrational, rotational, and translational motions. This is justified because the mass ratio of an electron to nucleus (m_{el}/m_{Nu}) is very small. A product form of the solutions of corresponding

Schrödinger equations therefore, represents a total wavefunction of the molecule. The electronic wavefunction is determined by an electronic Hamiltonian with fixed nuclei, and thus implicitly depends on the nuclear configuration (coordinates) as parameters. The eigenvalues obtained from the electronic Schrödinger equation also depend on the parameter, and are known as the adiabatic potential. On the other hand, the nuclear wavefunction describes motions of the nuclei in the resultant adiabatic potential. However, the BOA breaks down in the region of potential curve crossings, and experimental progresses [16] need more sophisticated theories beyond the BOA including the non-adiabatic effects explicitly.

Quite independently of problems concerning to the implementation of the BOA, there has been a debate on the relation between quantum mechanics and molecular structure. The discussion was initiated by Woolley[17]. The main theme of the debate was the impossibility of reconciling the notion of the molecular structure with quantum theory, because the molecular structure is a classical concept. Later, the most constructive critique of the BOA was provided by Essén[18]. The conclusion of his work was that the form of the Coulomb interaction, and not the smallness of the ratio m_{el}/m_{Nu}, is responsible for the approximate separation of collective and individual internal molecular motions. Although Essén did not provide a workable formalism, the resulting framework is very instructive. There exist many ideas and methods grounded on the Non Born-Oppenheimer (NBO) treatment for molecular systems in both static and dynamic cases [19]-[30]. Thomas and Joy applied the Hartree-Fock (HF) method not only to the electrons but also the protons, which are fermions with spin 1/2, and investigated the protonic spectra for several small molecules [19]. Pettitt discussed analogue of Koopmans' theorem for the protonic spectra [20]. Monkhorst presented a NBO molecular theory based upon the coupled cluster formalism for both time independent and dependent cases as an implementation of Essén's molecular theory. Lathouwers and co-workers applied the the generator coordinate method (GCM), which is originally introduced by Wheeller, Hill and Griffin in order to describe the collective motion in a nucleus [31],[32], to molecular systems and treated vibrational and rotational motions of hydrogen molecule non-adiabatically [30]. Recently, I have developed the NBO mean field method based upon the GCM [25] and have calculated molecular spectra and wavefunctions directly.

The non Born-Oppenheimer (NBO) treatments for molecular systems [21]-[26] have been presented by many workers. Particularly, the NBO density functional theory (NBO DFT) has been formulated by many authors, individually [21]-[23]. I proposed a numerical scheme that solves electron and nuclear coupled Kohn-Sham (KS) equations within the local spin density approximation(LSD) [26]. To reduce the many-body problem into the one-body picture based upon the KS theory makes the resulting total wavefunction separable into electronic and nuclear parts, which means that the KS theory is still under the BO regime. In order to overcome this difficulty, I need to go beyond the LSD and to improve on a treatment with the many-body effect.

The Green function method has been successful in providing efficient schemes for the accurate theoretical determination of many physical properties not only in solid state physics [33] but also in molecular physics [34]-[35]. The GW approximation (GWA), where the self-energy is a convolution over Green function G and effective interaction W, and related methods have been used largely in solid state such as the electron gas [36]-[37], conductors and insulators, metals [38], and atoms [39]. The accuracy of the GWA in these systems varies, though the results are better than those given by either the HF or the LSD.

In the present thesis, I present a calculation scheme for the NBO DFT based upon the Green function techniques within a static part of the GWA. The aim of this work is to examine an efficiency of this method. In chapter 2, I review the electron and nuclear coupled KS equations and present the detail of the NBO DFT formalism by means of the Green function techniques. I employ the GWA in order to develop the method beyond the LSD and to take account of the many-body effects. I discuss a basis set used here and consider its physical meaning. Numerical approach and programming algorithm are discussed in chapter 3. Chapter 4 concerns with the numerical examples of some physical properties of the individual motion in H_2 and μ_2. In chapter 5, the summary is presented.

Chapter 2

Theoretical background

First, the non Born-Oppenheimer(NBO) density functional theory, especially the electron and nuclear coupled Kohn-Sham(KS) equations, is briefly reviewed. A traditional density functional theory for electron is summarized in Appendix A [40]-[42]. The formulation of the coupled KS equations is an extension of the work by Gidopoulos [23] to multi-component systems. Next, I briefly explain the definition of NBO Green functions based upon the density functional formalism and formulate an expression for the generalization of the GWA to multi-component fermion systems. A summary of Green function method and the GW approximation are given in Appendix B. I also discuss the choice of basis used in this article and its physical meaning.

2.1 Overview of the NBO DFT: formalism and Kohn-Sham equation

The full Hamiltonian $\hat{H}$ for a molecular system consisting of N electrons and M nuclei is given as (atomic unit is used throughout in this text.)

$$\begin{aligned}\hat{H} &= -\frac{1}{2}\sum_{i}^{N}\nabla_i^2 - \sum_{a}^{M}\frac{1}{2m_a}\nabla_a^2 + \frac{1}{2}\sum_{i\neq j}^{N}\frac{1}{|\boldsymbol{r}_i-\boldsymbol{r}_j|} \\ &\quad + \frac{1}{2}\sum_{a\neq b}^{M}\frac{Z_aZ_b}{|\boldsymbol{R}_a-\boldsymbol{R}_b|} - \sum_{i}^{N}\sum_{a}^{M}\frac{Z_a}{|\boldsymbol{r}_i-\boldsymbol{R}_a|}\,, \end{aligned} \tag{2.1}$$

where $\boldsymbol{r}_i$ and $\boldsymbol{R}_a$ are the coordinate for i-th electron and for a-th nucleus, respectively. Z_a and m_a denote the atomic number of a-th nucleus and its mass. One defines one particle density for an electron with σ spin;

$$n_e^\sigma(\boldsymbol{r}_1) = \int d\tau |\Psi(\{\boldsymbol{r}_i,\sigma_i\},\{\boldsymbol{R}_a,I_a\})|^2\,, \tag{2.2}$$

and an α-type nucleus with I spin;

$$n_\alpha^I(\boldsymbol{R}_{\alpha_1}) = \int d\tau' |\Psi(\{\boldsymbol{r}_i,\sigma_i\},\{\boldsymbol{R}_a,I_a\})|^2\,, \tag{2.3}$$

where $\Psi(\{\boldsymbol{r}_i,\sigma_i\},\{\boldsymbol{R}_a,I_a\})$ is an exact ground state of a given system. $d\tau$ ($d\tau'$) denotes the product form of all spin-space volume element except for $d\sigma_1 d\boldsymbol{r}_1$ ($dI_1 d\boldsymbol{R}_{\alpha_1}$). Note that Greek indices (α, β, $\cdots$) denote types of nuclei, for example, a proton, a muon, and etc., whereas Roman indices (a, b, $\cdots$) in Eq.(2.1) denote an order corresponding to one nucleus.

I now define a ground state energy density functional for the NBO case as

$$E[\{\rho_e^\sigma\},\{\rho_\alpha^I\}] = \min\langle\Psi_{\{\rho_e^\sigma\},\{\rho_\alpha^I\}}|\hat{H}|\Psi_{\{\rho_e^\sigma\},\{\rho_\alpha^I\}}\rangle\,. \tag{2.4}$$

E searches all wave functions in the domain of the full Hamiltonian of Eq.(2.1) $\hat{H}$ of appropriate symmetries and the statistics of particles.

Next, I define two functionals as follows:

$$\tilde{E}[\{n_e^\sigma\},\{n_\alpha^I\}] = \min_{|\Psi\rangle\to(\{n_e^\sigma\},\{n_\alpha^I\})}\langle\Psi|T_e+T_n+V_{ee}+V_{nn}+V_{en}|\Psi\rangle\,, \tag{2.5}$$

$$E_0[\{n_e^\sigma\},\{n_\alpha^I\}] = \min_{|\chi\rangle\to\{n_\alpha^I\}}\langle\chi|T_n|\chi\rangle + \min_{|\phi\rangle\to\{n_e^\sigma\}}\langle\phi|T_e|\phi\rangle\,, \tag{2.6}$$

where the minimization of $\tilde{E}$ searches over all Ψ which is obtained from $(\{n_e^\sigma\},\{n_\alpha^I\})$, while the minimization of E_0 searches over a N-particle Slater determinant for electrons, $|\phi\rangle$, and the product of M_α-particle Slater determinants for fermion nuclei and/or permanents for boson nuclei, $|\chi\rangle$, which are obtained from $(\{n_e^\sigma\},\{n_\alpha^I\})$, as

$$|\phi\rangle = \det|\,\{\phi_i^{e\sigma}(\boldsymbol{r})\}\,|\,, \tag{2.7}$$

$$|\chi\rangle = \prod_\alpha|\chi_\alpha\rangle, \tag{2.8}$$

with

$$|\chi_\alpha\rangle = \begin{cases}\det|\left\{\chi_i^{\alpha I}(\boldsymbol{R})\right\}| & \text{(for fermion nucleus)}\,,\\ \mathrm{per}|\left\{\chi_i^{\alpha I}(\boldsymbol{R})\right\}| & \text{(for boson nucleus)}\,,\end{cases} \tag{2.9}$$

where det and per mean the determinant for the fermion and the permanent for the boson, respectively. $M_\alpha (M = \sum_\alpha M_\alpha)$ denotes the number of the α nucleus in a given system.

I assume that there is a state which minimize the above functionals. I define $\Psi_{\{n_e^\sigma\},\{n_\alpha^I\}}$, $\chi_{n_\alpha^I}$, and $\phi_{n_e^\sigma}$ which minimize above functionals.

$$\tilde{E}[\{n_e^\sigma\},\{n_\alpha^I\}] = \langle \Psi_{\{n_e^\sigma\},\{n_\alpha^I\}} | T_e + T_n + V_{ee} + V_{nn} + V_{en} | \Psi_{\{n_e^\sigma\},\{n_\alpha^I\}} \rangle \,, \tag{2.10}$$

$$E_0[\{n_e^\sigma\},\{n_\alpha^I\}] = \langle \chi_{\{n_\alpha^I\}} | T_n | \chi_{\{n_\alpha^I\}} \rangle + \langle \phi_{\{n_e^\sigma\}} | T_e | \phi_{\{n_e^\sigma\}} \rangle \,. \tag{2.11}$$

I now define the exchange-correlation energy functional as

$$\begin{aligned} E_{xc}[\{n_e^\sigma\},\{n_\alpha^I\}] &= \tilde{E}[\{n_e^\sigma\},\{n_\alpha^I\}] - E_0[\{n_e^\sigma\},\{n_\alpha^I\}] \\ &- \frac{1}{2}\int\int d\boldsymbol{r} d\boldsymbol{r}' \frac{\sum_\sigma n_e^\sigma(\boldsymbol{r}) \sum_\rho n_e^\rho(\boldsymbol{r}')}{|\boldsymbol{r}-\boldsymbol{r}'|} \\ &- \frac{1}{2}\sum_{\alpha\beta} Z_\alpha Z_\beta \int\int d\boldsymbol{R} d\boldsymbol{R}' \frac{\sum_I n_\alpha^I(\boldsymbol{R}) \sum_J n_\beta^J(\boldsymbol{R}')}{|\boldsymbol{R}-\boldsymbol{R}'|} \\ &+ \sum_\alpha Z_\alpha \int\int d\boldsymbol{r} d\boldsymbol{R} \frac{\sum_\sigma n_e^\sigma(\boldsymbol{r}) \sum_I n_\alpha^I(\boldsymbol{R})}{|\boldsymbol{r}-\boldsymbol{R}|} \,. \end{aligned} \tag{2.12}$$

I obtain the KS functional for the molecular system as

$$\begin{aligned} E[\phi,\chi] &= \langle\chi|\langle\phi|T_e + T_n|\chi\rangle|\phi\rangle + E_{xc}[\{n_e^\sigma\},\{n_\alpha^I\}] \\ &+ \frac{1}{2}\int\int d\boldsymbol{r} d\boldsymbol{r}' \frac{\sum_\sigma n_e^\sigma(\boldsymbol{r}) \sum_\rho n_e^\rho(\boldsymbol{r}')}{|\boldsymbol{r}-\boldsymbol{r}'|} \\ &+ \frac{1}{2}\sum_{\alpha\beta} Z_\alpha Z_\beta \int\int d\boldsymbol{R} d\boldsymbol{R}' \frac{\sum_I n_\alpha^I(\boldsymbol{R}) \sum_J n_\beta^J(\boldsymbol{R}')}{|\boldsymbol{R}-\boldsymbol{R}'|} \\ &- \sum_\alpha Z_\alpha \int\int d\boldsymbol{r} d\boldsymbol{R} \frac{\sum_\sigma n_e^\sigma(\boldsymbol{r}) \sum_I n_\alpha^I(\boldsymbol{R})}{|\boldsymbol{r}-\boldsymbol{R}|} \,. \end{aligned} \tag{2.13}$$

$E[\phi,\chi]$ is the functional of orbitals ϕ_i^σ and $\chi_j^{\alpha I}$, because noninteracting states ϕ and χ are constructed by the Slater determinants or permanents which consists the orbitals ϕ_i^σ and $\chi_j^{\alpha I}$. If the orbitals minimize the functional, I obtain the electron and nuclear coupled KS equations (CKSE) as

$$\begin{aligned} F^{e\sigma}\phi_i^\sigma(\boldsymbol{r}) &= \left[-\frac{\nabla^2}{2} + v_{xc}^\sigma[\{n_e^\sigma\},\{n_\alpha^I\}](\boldsymbol{r}) + V_H(\boldsymbol{r})\right]\phi_i^\sigma(\boldsymbol{r}) \\ &= \varepsilon_i^\sigma \phi_i^\sigma(\boldsymbol{r}) \,, \end{aligned} \tag{2.14}$$

$$\begin{aligned} F^{\alpha I}\chi_i^{\alpha I}(\boldsymbol{R}) &= \left[-\frac{\nabla^2}{2M_\alpha} + V_{xc}^{\alpha I}[\{n_e^\sigma\},\{n_\alpha^I\}](\boldsymbol{R}) - Z_\alpha V_H(\boldsymbol{R})\right]\chi_i^{\alpha I}(\boldsymbol{R}) \\ &= E_i^{\alpha I}\chi_i^{\alpha I}(\boldsymbol{R}) \,, \end{aligned} \tag{2.15}$$

where $F^{e\sigma}(F^{\alpha I})$ and $\varepsilon_i^\sigma(E_i^{\alpha I})$ are the KS operator and corresponding i-th eigenvalue for the electron with the spin σ(the α nucleus with the spin I) and depend on their spin. The classical Coulomb potential (Hartree potential) is given by

$$V_H(\boldsymbol{r}) = \int d\boldsymbol{r}' \left[\frac{\sum_\sigma n_e^\sigma(\boldsymbol{r}')}{|\boldsymbol{r}-\boldsymbol{r}'|} - \sum_\alpha Z_\alpha \frac{\sum_I n_\alpha^I(\boldsymbol{r}')}{|\boldsymbol{r}-\boldsymbol{r}'|}\right] . \tag{2.16}$$

The exchange-correlation potential for the electron and nucleus are defined as

$$v_{xc}^\sigma[\{n_e^\sigma\},\{n_\alpha^I\}] = \frac{\delta E_{xc}[\{n_e^\sigma\},\{n_\alpha^I\}]}{\delta n_e^\sigma} \,, \tag{2.17}$$

$$V_{xc}^{\alpha I}[\{n_e^\sigma\},\{n_\alpha^I\}] = \frac{\delta E_{xc}[\{n_e^\sigma\},\{n_\alpha^I\}]}{\delta n_\alpha^I} \,, \tag{2.18}$$

where n_e^σ and n_α^I denote the densities of electron and nucleus, respectively, as follows:

$$n_e^\sigma(\boldsymbol{r}) = \sum_{i=1}^{N} |\phi_i^\sigma(\boldsymbol{r})|^2 \,, \tag{2.19}$$

$$n_\alpha^I(\boldsymbol{R}) = \sum_{j=1}^{M_\alpha} |\chi_j^{\alpha I}(\boldsymbol{R})|^2 \,. \tag{2.20}$$

2.2 Definition of Green functions in NBO regime

In order to introduce the one-particle Green function, I here use the second quantized formalism. The full Hamiltonian is expressed as

$$\begin{aligned} \hat{H} &= \sum_\sigma \int d^3\boldsymbol{x}\, \hat{\psi}_\sigma^\dagger(\boldsymbol{x}) \left[-\frac{\nabla^2}{2}\right] \hat{\psi}_\sigma(\boldsymbol{x}) + \sum_\alpha \sum_I \int d^3\boldsymbol{R}\, \hat{\phi}_{\alpha I}^\dagger(\boldsymbol{R}) \left[-\frac{\nabla^2}{2m_\alpha}\right] \hat{\phi}_{\alpha I}(\boldsymbol{R}) \\ &+ \frac{1}{2}\sum_{\sigma\rho} \int d^3\boldsymbol{x} \int d^3\boldsymbol{x}'\, \hat{\psi}_\sigma^\dagger(\boldsymbol{x}) \hat{\psi}_\rho^\dagger(\boldsymbol{x}') \frac{1}{|\boldsymbol{r}-\boldsymbol{r}'|} \hat{\psi}_\rho(\boldsymbol{x}') \hat{\psi}_\sigma(\boldsymbol{x}) \\ &+ \frac{1}{2}\sum_{\alpha,\beta} \sum_{IJ} \int d^3\boldsymbol{R} \int d^3\boldsymbol{R}'\, \hat{\phi}_{\alpha I}^\dagger(\boldsymbol{R}) \hat{\phi}_{\beta J}^\dagger(\boldsymbol{R}') \frac{Z_\alpha Z_\beta}{|\boldsymbol{R}-\boldsymbol{R}'|} \hat{\phi}_{\beta J}(\boldsymbol{R}') \hat{\phi}_{\alpha I}(\boldsymbol{R}) \\ &- \sum_\alpha \sum_I \sum_\sigma \int d^3\boldsymbol{x} \int d^3\boldsymbol{R}\, \hat{\psi}_\sigma^\dagger(\boldsymbol{x}) \hat{\phi}_{\alpha I}^\dagger(\boldsymbol{R}) \frac{Z_\alpha}{|\boldsymbol{x}-\boldsymbol{R}|} \hat{\phi}_{\alpha I}(\boldsymbol{R}) \hat{\psi}_\sigma(\boldsymbol{x}) \,, \end{aligned} \tag{2.21}$$

where $\hat{\psi}_\sigma^\dagger(\boldsymbol{x})(\hat{\psi}_\sigma(\boldsymbol{x}))$ and $\hat{\phi}_{\alpha I}^\dagger(\boldsymbol{R})(\hat{\phi}_{\alpha I}(\boldsymbol{R}))$ are the creation(or annihilation) operators for an electron with spin σ and a nucleus α with spin I, respectively. They satisfy the

ordinary or anti- commutation relation depending upon their statistics.

$$\begin{aligned}\left[\hat{\psi}_\sigma(\boldsymbol{x}t),\hat{\psi}^\dagger_\rho(\boldsymbol{x}'t')\right]_+ &= \delta(\boldsymbol{x}-\boldsymbol{x}')\delta(t-t')\delta_{\sigma\rho}\,,\\ \left[\hat{\phi}_{\alpha I}(\boldsymbol{R}t),\hat{\phi}^\dagger_{\beta I'}(\boldsymbol{R}'t')\right]_\pm &= \delta(\boldsymbol{R}-\boldsymbol{R}')\delta(t-t')\delta_{\alpha\beta}\delta_{II'}\,,\\ \left[\hat{\psi}_\sigma(\boldsymbol{x}t),\hat{\psi}_\rho(\boldsymbol{x}'t')\right]_+ &= \left[\hat{\phi}_{\alpha I}(\boldsymbol{x}t),\hat{\phi}_{\beta I'}(\boldsymbol{x}'t')\right]_\pm = \cdots = 0\,,\end{aligned} \tag{2.22}$$

where (-) sign denotes the ordinary commutation relation for the bosons, while (+) sign denotes the anti-commutation relation for the fermions. I assume that the bose condensation dose not occur even at zero temperature.

The single-particle Green functions for those particles are defined in terms of these creation and annihilation operators in the Heisenberg representation as

$$G^e(\boldsymbol{x}t,\boldsymbol{x}'t')^{\sigma\rho} = -i\langle\Psi_{N,M}|T[\hat{\psi}_\sigma(\boldsymbol{x}t)\hat{\psi}^\dagger_\rho(\boldsymbol{x}'t')]|\Psi_{N,M}\rangle\,, \tag{2.23}$$

$$G^\alpha(\boldsymbol{R}t,\boldsymbol{R}'t')^{IJ} = -i\langle\Psi_{N,M}|T[\hat{\phi}_{\alpha I}(\boldsymbol{R}t)\hat{\phi}^\dagger_{\alpha J}(\boldsymbol{R}'t')]|\Psi_{N,M}\rangle\,, \tag{2.24}$$

where $T[\cdots]$ denotes the time ordering product. $|\Psi_{N,M}\rangle$ is the exact ground state in the Heisenberg representation for the interacting molecular system and obeys the Schrödinger equation

$$\hat{H}|\Psi_{N,M}\rangle = E|\Psi_{N,M}\rangle\,. \tag{2.25}$$

The creation and annihilation operators for the electron obey the equation of motion

$$i\frac{\partial\hat{\psi}^{(\dagger)}_\sigma(\boldsymbol{x}t)}{\partial t} = \left[\hat{\psi}^{(\dagger)}_\sigma(\boldsymbol{x}t),\hat{H}\right]_+\,. \tag{2.26}$$

Note that the creation and annihilation operators for the nuclei obey the same equation.

By means of the definition of the Green functions of Eqs.(2.23) and (2.24), the equation of motion of Eq.(2.26), and the Hamiltonian of Eq.(2.21), I obtain coupled Dyson equations

$$\begin{aligned}\left[i\frac{\partial}{\partial t}+\frac{\nabla^2}{2}\right]G^e(\boldsymbol{x}t,\boldsymbol{x}'t')^{\sigma\rho} &= \delta(\boldsymbol{x}-\boldsymbol{x}')\delta(t-t')\delta_{\sigma\rho}\\ &+ i\sum_\lambda\int d^3\boldsymbol{y}V_{ee}(\boldsymbol{x},\boldsymbol{y})^{(2)}G^{ee}(\boldsymbol{x}t,\boldsymbol{y}t,\boldsymbol{x}'t',\boldsymbol{y}t^+)^{\sigma\lambda;\rho\lambda}\\ &+ i\sum_{\alpha I}\int d^3\boldsymbol{R}V_{e\alpha}(\boldsymbol{x},R)^{(2)}G^{e\alpha}(\boldsymbol{x}t,\boldsymbol{R}t,\boldsymbol{x}'t',\boldsymbol{R}t^+)^{\sigma I;\rho I}\end{aligned}\,, \tag{2.27}$$

where the 2-body Green function for the electron is defined as

$$\begin{aligned}&{}^{(2)}G^{ee}(\boldsymbol{x}_1t_1,\boldsymbol{x}_2t_2,\boldsymbol{x}_1't_1',\boldsymbol{x}_2t_2')^{\sigma\lambda;\rho\lambda}\\ &= (-i)^2\langle\Psi_{N,M}|T[\hat{\psi}_\sigma(\boldsymbol{x}_1t_1)\hat{\psi}_\lambda(\boldsymbol{x}_2t_2)\hat{\psi}^\dagger_\rho(\boldsymbol{x}_2't_2')\hat{\psi}^\dagger_\lambda(\boldsymbol{x}_1't_1')]|\Psi_{N,M}\rangle\,.\end{aligned} \tag{2.28}$$

The 2-body Green function for the electron interacting with α particle is defined as

$$\begin{aligned}&{}^{(2)}G^{e\alpha}(\boldsymbol{x}_1t_1,\boldsymbol{R}_2t_2,\boldsymbol{x}_1't_1',\boldsymbol{R}_2't_2')^{\sigma I;\rho J}\\ &= (-i)^2\langle\Psi_{N,M}|T[\hat{\psi}_\sigma(\boldsymbol{x}_1t_1)\hat{\phi}_{\alpha I}(\boldsymbol{R}_2t_2)\hat{\phi}^\dagger_{\alpha J}(\boldsymbol{R}_2't_2')\hat{\psi}^\dagger_\rho(\boldsymbol{x}_1't_1')]|\Psi_{N,M}\rangle\,.\end{aligned} \tag{2.29}$$

Self-energy Σ is defined through the following Dyson equation

$$\begin{aligned}\left[i\frac{\partial}{\partial t}+\frac{\nabla^2}{2}\right]G^e(\boldsymbol{x}t,\boldsymbol{x}'t')^{\sigma\rho} &= \delta(\boldsymbol{x}-\boldsymbol{x}')\delta(t-t')\delta_{\sigma\rho}\\ &+ i\sum_\lambda\int d^3\boldsymbol{y}dt_1\Sigma^{ee}(\boldsymbol{x}t,\boldsymbol{y}t_1)^{\sigma\lambda}G^e(\boldsymbol{y}t_1,\boldsymbol{x}'t')^{\lambda\rho}\\ &+ i\sum_\lambda\sum_\alpha\int d^3\boldsymbol{y}dt_1\Sigma^{e\alpha}(\boldsymbol{x}t,\boldsymbol{y}t_1)^{\sigma\lambda}G^e(\boldsymbol{y}t_1,\boldsymbol{x}'t')^{\lambda\rho}\,,\end{aligned} \tag{2.30}$$

These equations hold for the nuclear Green functions as

$$\begin{aligned}\left[i\frac{\partial}{\partial t}+\frac{\nabla^2}{2m_\alpha}\right]G^\alpha(\boldsymbol{x}t,\boldsymbol{x}'t')^{II'} &= \delta(\boldsymbol{x}-\boldsymbol{x}')\delta(t-t')\delta_{II'}\\ &+ i\sum_J\sum_\beta\int d^3\boldsymbol{y}dt_1\Sigma^{\alpha\beta}(\boldsymbol{x}t,\boldsymbol{y}t_1)^{IJ}G^\alpha(\boldsymbol{y}t_1,\boldsymbol{x}'t')^{JI'}\\ &+ i\int d^3\boldsymbol{y}dt_1\Sigma^{\alpha e}(\boldsymbol{x}t,\boldsymbol{y}t_1)^{IJ}G^\alpha(\boldsymbol{y}t_1,\boldsymbol{x}'t')^{JI'}\,.\end{aligned} \tag{2.31}$$

I call these equation electron and nuclear coupled Dyson equations because of cross terms $\Sigma^{e\alpha}$ and $\Sigma^{\alpha e}$ in Eqs(2.27) and (2.31). As the Hamiltonian of Eq.(2.21) is independent of time, I can carry out the Fourier transformation with respect to time for the above formula, then obtain

$$\begin{aligned}\left[\omega+\frac{\nabla_1^2}{2}\right]G^e(1,2,\omega)^{\sigma\rho} &= \delta(1,2)\delta_{\sigma\rho}+\int d^3(3)\sum_\lambda\\ &\times\left(\Sigma^{ee}(1,3,\omega)^{\sigma\lambda}+\sum_\alpha\Sigma^{e\alpha}(1,3,\omega)^{\sigma\lambda}\right)G^e(3,2,\omega)^{\lambda\rho}\,,\end{aligned} \tag{2.32}$$

$$\left[\omega+\frac{\nabla_1^2}{2m_\alpha}\right]G^\alpha(1,2,\omega)^{II'} = \delta(1,2)\delta_{II'}+\int d^3(3)\sum_J \times\left(\sum_\beta \Sigma^{\alpha\beta}(1,3)^{IJ}+\Sigma^{\alpha e}(1,3)^{IJ}\right)G^\alpha(3,2,\omega)^{JI'} . \tag{2.33}$$

I here use abbreviations for the coordinate, $(1)=(\boldsymbol{x}_1)$.

By definition, zero-th order Green functions are given by the solution of following equations:

$$\left[\omega+\frac{\nabla_1^2}{2}\right]G^{e(0)}(1,2,\omega)^{\sigma\rho} = \delta(1,2)\delta_{\sigma\rho} , \tag{2.34}$$

$$\left[\omega+\frac{\nabla_1^2}{2m_\alpha}\right]G^{\alpha(0)}(1,2,\omega)^{II'} = \delta(1,2)\delta_{II'} . \tag{2.35}$$

By means of the zero-th order Green functions, the coupled Dyson equations become

$$G^e(1,2,w)^{\sigma\rho} = G^{e(0)}(1,2,w)^{\sigma\sigma}\delta_{\sigma\rho}+\sum_\lambda\int d(3)d(4)G^{e(0)}(1,3,w)^{\sigma\sigma} \times\left[\Sigma^{ee}(3,4,w)^{\sigma\lambda}+\sum_\alpha\Sigma^{e\alpha}(3,4,w)^{\sigma\lambda}\right]G^e(4,2,w)^{\lambda\rho} , \tag{2.36}$$

$$G^\alpha(1,2,w)^{II'} = G^{\alpha(0)}(1,2,w)^{II}\delta_{II'}+\sum_J\int d(3)d(4)G^{\alpha(0)}(1,3,w)^{II} \times\left[\Sigma^{\alpha e}(3,4,w)^{IJ}+\sum_\beta\Sigma^{\alpha\beta}(3,4,w)^{IJ}\right]G^\alpha(4,2,w)^{JI'} . \tag{2.37}$$

Therefore, a main problem is now reduced to calculate the self-energy Σ.

Although I choose the zero-th order Green function as the solutions of the non-interacting free particles, in general, the choice of the zero-th order Green functions is arbitrary. For example, I can use those of the non-interacting free particles, of the Hartree or the Hartree-Fock approximation, and of the local spin density(LSD) approximation. In this work, I adopt those of the LSD. I rewrite the coupled Dyson equations within the LSD as

$$G^e(1,2,w)^{\sigma\rho} = g^e(1,2,w)^{\sigma\sigma}\delta_{\sigma\rho}+\sum_\lambda\int d(3)d(4)g^e(1,3,w)^{\sigma\sigma} \times\left[\Delta\Sigma^{ee}(3,4,w)^{\sigma\lambda}+\sum_\alpha\Delta\Sigma^{e\alpha}(3,4,w)^{\sigma\lambda}\right]G^e(4,2,w)^{\lambda\rho} , \tag{2.38}$$

$$G^\alpha(1,2,w)^{II'} = g^\alpha(1,2,w)^{II}\delta_{II'}+\sum_J\int d(3)d(4)g^\alpha(1,3,w)^{II} \times\left[\Delta\Sigma^{\alpha e}(3,4,w)^{IJ}+\sum_\beta\Delta\Sigma^{\alpha\beta}(3,4,w)^{IJ}\right]G^\alpha(4,2,w)^{JI'} , \tag{2.39}$$

where g^e and g^α are non-interacting Green functions for the electron and for the nucleus α within the LSD, respectively, and obey the coupled KS equations

$$\left[\omega+F^{e\sigma}\right]g^e(1,2,w)^{\sigma\sigma} = 0 , \tag{2.40}$$

$$\left[\omega+F^{\alpha I}\right]g^\alpha(1,2,w)^{II} = 0 , \tag{2.41}$$

where $F^{e\sigma}$ and $F^{\alpha I}$ are the KS operators appearing in Eqs(2.14) and (2.15), and the one particle densities are evaluated by means of the Green functions

$$n_e^\sigma(1) = g^e(1,1,w\to 0)^{\sigma\sigma} ,$$

$$n_\alpha^I(1) = g^\alpha(1,1,w\to 0)^{II} . \tag{2.42}$$

$\Delta\Sigma$ represents a self-energy within the LSD

$$\Delta\Sigma^{ab}=\Sigma^{ab}-V_H^{ab}-v_{xc}^a\delta_{ab} , \tag{2.43}$$

where Σ^{ab} denotes the proper self-energy of a particle a interacting with a particle b, V_H^{ab} is the classical Coulomb potential between particles a and b, and v_{xc}^a is the exchange-correlation potential of the particle a within the LSD. Note that the indices for types of particles (a, b, $\cdots$) include both the electron(e) and nuclei(α, β, $\cdots$).

The noninteracting Green functions g^e and g^α are, then, expressed in terms of the KS orbitals and its eigenvalues:

$$g^e(1,2,w)^{\sigma\rho} = \left[\sum_j^{occ}\frac{\phi_j^{\sigma*}(1)\phi_j^\sigma(2)}{w-\varepsilon_j^\sigma-i\eta}+\sum_j^{unocc}\frac{\phi_j^{\sigma*}(1)\phi_j^\sigma(2)}{w-\varepsilon_j^\sigma+i\eta}\right]\delta_{\sigma\rho} ,$$

$$g^\alpha(1,2,w)^{II'} = \left[\sum_j^{occ}\frac{\chi_j^{\alpha I*}(1)\chi_j^{\alpha I}(2)}{w-E_j^{\alpha I}-i\eta}+\sum_j^{unocc}\frac{\chi_j^{\alpha I*}(1)\chi_j^{\alpha I}(2)}{w-E_j^{\alpha I}+i\eta}\right]\delta_{II'} . \tag{2.44}$$

In what follows, I use the matrix representation such as $\boldsymbol{G}$, $\boldsymbol{g}$, and $\boldsymbol{\Delta\Sigma}$ whose elements are $\langle i|G|j\rangle$, $\langle i|g|j\rangle$, and $\langle i|\Delta\Sigma|j\rangle$, respectively.

So far, I formulate the coupled Dyson equations for both fermi and bose particles. Although there exist many bose nuclei, I restrict ourselves on treating multi-fermion systems for simplicity. Derivation for the bose nuclei will be done in a future article.

2.3 GW approximation for multi-component fermion systems

I next introduce the GWA that was first developed by Hedin [36]-[37]. The GWA is derived systematically from the many-body perturbation theory. Many applications to wide class of systems in solid state physics have been reported [38]. I here extend the GWA to multi-component fermi systems treated in previous section.

Within the simplest GWA, the self-energy $\Delta\boldsymbol{\Sigma}$ and the polarization function $\boldsymbol{P}$ are approximated as

$$\Delta\boldsymbol{\Sigma}^{ab}(\omega) = \int \frac{d\omega'}{2\pi}\boldsymbol{W}^{ab}(\omega')\boldsymbol{G}^{a}(\omega+\omega') , \tag{2.45}$$

$$\boldsymbol{P}^{aa}(\omega) = \int \frac{d\omega'}{2\pi}\boldsymbol{G}^{a}(\omega')\boldsymbol{G}^{a}(\omega+\omega') . \tag{2.46}$$

where $\boldsymbol{W}$ is the matrix form of the screened Coulomb interaction defined as

$$\begin{aligned}\boldsymbol{W}^{ab}(\omega) &= \boldsymbol{V}^{aa}\delta_{ab} + \boldsymbol{V}^{ab}\boldsymbol{P}^{bb}(\omega)(\boldsymbol{V}^{ab})^{\dagger} \\ &\quad + \boldsymbol{V}^{aa}\boldsymbol{P}^{aa}(\omega)\boldsymbol{V}^{ab}\boldsymbol{P}^{bb}(\omega)(\boldsymbol{V}^{ab})^{\dagger}(1-\delta_{ab}) \\ &\quad + \boldsymbol{V}^{ab}\boldsymbol{P}^{bb}(\omega)(\boldsymbol{V}^{ab})^{\dagger}\boldsymbol{P}^{aa}(\omega)\boldsymbol{V}^{aa}(1-\delta_{ab}) .\end{aligned} \tag{2.47}$$

Note that $\boldsymbol{W}$, $\boldsymbol{V}$, and $\boldsymbol{P}$ are four-component supermatrices in contrast to $\boldsymbol{G}$, $\boldsymbol{g}$, and $\Delta\boldsymbol{\Sigma}$, which are ordinary matrices.

Using zero-th order polarization functions $\boldsymbol{p}$, which are obtained from Eq.(2.46) with the noninteracting Green functions $\boldsymbol{g}$, the coupled Dyson equations for the polarization functions are given as

$$(\boldsymbol{P}^{aa}(\omega))^{-1} = (\boldsymbol{p}^{aa}(\omega))^{-1} - \left(\boldsymbol{V}^{aa} + \sum_{b\neq a}\boldsymbol{W}^{ab(0)}(\omega)\right) , \tag{2.48}$$

where $\boldsymbol{W}^{ab(0)}$ is obtained from substituting $\boldsymbol{P}^{aa(0)}$, which is defined as

$$\left(\boldsymbol{P}^{aa(0)}(\omega)\right)^{-1} = (\boldsymbol{p}^{aa}(\omega))^{-1} - \boldsymbol{V}^{aa} , \tag{2.49}$$

for Eq.(2.47). Although these equations are solved self-consistently, I truncate the iteration in actual calculations.

In order to clarify the terms appearing in the GWA for two component fermion systems, I analyze the structure of the GWA by using the Feynmann diagrams. The diagram expansion of the GWA for the electron is illustrated in Fig.2.1. Here, the zero-th order Green functions for both the electron g^{e} and nucleus g^{α} are denoted by a straight line and dashed line with an arrow, respectively, where the arrow shows the direction of propagation. On the other hand, a straight wavy line and dashed wavy line denote the bare Coulomb interactions for electron-electron(e-e) V^{ee} and nucleus-nucleus(n-n) $V^{\alpha\alpha}$, respectively, and a dashed line without an arrow is the Coulomb interaction between electron and nucleus(e-n) $V^{e\alpha}$. In the traditional framework, only (a) type diagrams are included. On the other hand, I include (b) and (c) type diagrams in the formulation. The diagrams (a) come from first term and second term in Eq.(2.47) when $a = b$. The diagrams (b) and (c) come, respectively, from second and third term in Eq.(2.47) when $a \neq b$. Those for the nucleus are obtained by alternating g^{e} to g^{α} and V^{ee} to $V^{\alpha\alpha}$.

Moreover, I restrict myself on treating the static limit of the GWA as the self-energy. This approximation is known as the static COHSEX(coulomb hole and static exchange) approximation, which was first introduced by Hedin in order to investigate the static properties of homogeneous electron gas, and reliable for the states close to the Fermi level. With the approximation, the real part of self-energies becomes

$$\begin{aligned}\mathrm{Re}\Delta\boldsymbol{\Sigma}^{ab}(\omega)^{SEX} &= -\mathrm{Re}\sum_{k}^{occ}\boldsymbol{W}^{ab}(\omega-\epsilon_k) , \\ \mathrm{Re}\Delta\boldsymbol{\Sigma}^{ab}(\omega)^{SCOH} &= \mathrm{Re}(\boldsymbol{W}^{ab}(0)-\boldsymbol{V}^{ab}) .\end{aligned} \tag{2.50}$$

In these equation, SEX and SCOH mean the "screened exchange" and the "static coulomb hole", respectively.

2.4 Choice of basis set

According to the Essén's view of molecules [18], where the motion of a whole system is separated into the translational, the individual and collective motions, I start with a coordinate transformation for the classical Hamiltonian. Since I am interested in internal motions in a molecule, I first eliminate the translational motion from the Hamiltonian.

To avoid introducing independent variables, I impose some conditions as follows. New coordinates are defined with two conditions as

$$\boldsymbol{r}_i = \boldsymbol{r}^G + \boldsymbol{r}^C_{\gamma(i)} + \boldsymbol{r}^I_i \qquad (i = 1, \cdots, N+M)\,, \tag{2.51}$$

$$0 = \sum_{\gamma(i)} m_i \boldsymbol{r}^I_i \qquad (p = 1, \cdots, M)\,, \tag{2.52}$$

$$0 = \sum_{p=1}^{M} m_p \boldsymbol{r}^C_p \qquad (m_p = \sum_{\gamma(i)=p} m_i)\,, \tag{2.53}$$

where $\boldsymbol{r}^G$, $\boldsymbol{r}^C_{\gamma(i)}$, and $\boldsymbol{r}^I_i$ are the coordinate of the center of mass(COM) for a whole system, that of COM for a subsystem(atom) p, and that of individual motion, respectively. The superscripts of G, C, respectively, and I denote "center of mass for a whole system", "collective motion", and "individual motion", hereafter. $\gamma(i)$ represents a subsystem in which particle i is inherent. The velocity of particle i can be written by

$$\boldsymbol{v}_i = \boldsymbol{v}^G + \boldsymbol{v}^C_{\gamma(i)} + \boldsymbol{v}^I_i\,, \tag{2.54}$$

and the classical kinetic energy becomes

$$\begin{aligned} T &= \frac{1}{2}\sum_i^{N+M} m_i \boldsymbol{v}_i^2 \\ &= \frac{1}{2} M_G \boldsymbol{v}_G^2 + \frac{1}{2}\sum_p^M m_p \left(\boldsymbol{v}^C_p\right)^2 + \frac{1}{2}\sum_i^{N+M} m_i \left(\boldsymbol{v}^I_i\right)^2 + T^{GC} + T^{GI} + T^{CI}\,, \end{aligned} \tag{2.55}$$

where M_G is total mass of the system. From the conditions, cross terms of T^{GC}, T^{GI}, and T^{CI} in the right hand of Eq.(2.55) become identically zero for the classical case. I can now write the kinetic energy of the internal motions in the molecule:

$$T_{int} = \frac{1}{2}\sum_\alpha^M m_p \left(\boldsymbol{v}^C_p\right)^2 + \frac{1}{2}\sum_i^{N+M} m_i \left(\boldsymbol{v}^I_i\right)^2\,, \tag{2.56}$$

In analogous to the ordinary canonical commutation relation between a coordinate and a momentum, the kinetic energy operator of the internal motion in a quantum mechanical form is approximated as

$$T_{int} = -\frac{1}{2}\sum_p^M \frac{\left(\nabla^C_p\right)^2}{m_p} - \frac{1}{2}\sum_i^{N+M} \frac{\left(\nabla^I_i\right)^2}{m_i}\,, \tag{2.57}$$

Although Eq.(2.57) does not strictly hold in the quantum case because of the cross terms, I neglect the cross terms as a first approximation.

I next introduce approximate one particle wavefunctions for an electron and nuclei as

$$\begin{aligned} \phi(\boldsymbol{r}) &\approx \sum_p C^{e\sigma}_p \phi(\boldsymbol{r} - \boldsymbol{r}^C_p)\,, \\ \chi(\boldsymbol{R}) &\approx \sum_p C^{\alpha I}_p \chi(\boldsymbol{R} - \boldsymbol{r}^C_p)\,, \end{aligned} \tag{2.58}$$

where $\boldsymbol{r}^C_p$ are approximated to be set on the position of atom p, and C denotes an expansion coefficient determined from the variational principle. Here, the position of COM for the whole system $\boldsymbol{r}^G$ is implicitly set at origin. These basis sets physically represent the individual motions of particles in the molecular system.

In actual calculations, I use the Gaussian basis set whose center is $\tilde{\boldsymbol{r}}^C_p$, for both ϕ and χ. I assume that the centers of the Gaussian are treated as parameters $\tilde{\boldsymbol{r}}^C_p$, which are also determined by the variational principle minimizing the total energy, and that only the kinetic energy operator for the individual motions acts on the basis. These assumptions imply that the equations to be solved are those for internal motions around atoms with relatively small variations. Then, the method may be inappropriate for describing the dynamical collective motions such as the large amplitude vibrational motion, i.e., the inversion of NH_3 umbrella. The basis depending on the centers leads to the analogy to the nonadiabatic effect. Extension to include the nonadiabatic correlation will be considered in future works.

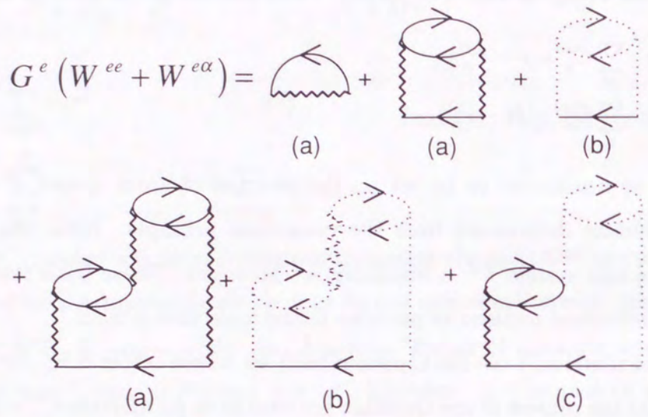

+ Higher order terms

Figure 2.1: Dyagramatic expression of GWA for electron. (a), (b) and (c) denote type of the Feynman diagrams.

Chapter 3

Numerical approach

Here I give details of a calculation scheme of the density functional method discussed above. I first explain the manner of the self consistent field method for coupled systems of electron and nuclei, i.e. I call it coupled Kohn-Sham equations(CKSE) as an extension of traditional unrestricted Hartree-Fock approach, secondly a numerical treatment with exchange-correlation potentials appearing in the CKSE [44].

3.1 Self Consistent field method for coupled Kohn-Sham equations

I here discuss calculation method for solving the CKSE by using the linear combination of molecular orbital (LCAO) method. Note that spin indices are neglected for simplicity. The extension of including spin variables is quite easy.

By expanding the molecular orbital using a set of known basis functions $\{f_i\}$ $(i = 1, 2, \cdots, K)$ as

$$\begin{aligned} \phi_i(\boldsymbol{r}) &= \sum_r^K C_{ir} f_r(\boldsymbol{r}) \,, \\ \chi_i^\alpha(\boldsymbol{R}) &= \sum_r^K C_{ir}^\alpha f_r(\boldsymbol{r}) \,, \end{aligned} \tag{3.1}$$

where K denotes a number of a basis set. In general, K for electron can differ form that for nucleus. For simplicity, I use the same number of the basis. From Eqs.(2.14), (2.15),

and (3.1), the problem of calculation the coupled Kohn-Sham equation reduced to the problem of calculating the set of expansion coefficients $[\{C^e\}, \{C^\alpha\}]$.

By substituting the linear expansion Eq.(3.1) into the CKSE, I obtain a matrix equation for the expansion coefficients $[\{C^e\}, \{C^\alpha\}]$ as

$$\sum_s (F^e_{rs} - \varepsilon^\sigma_i S^e_{rs})\, C^e_{is} = 0\,, \tag{3.2}$$

$$\sum_s \left(F^\alpha_{rs} - E^{\alpha I}_i S^\alpha_{rs}\right) C^\alpha_{is} = 0\,, \tag{3.3}$$

where ε_i and E_i are i-th orbital energy for electron and nucleus, respectively, and F_{rs} and S_{rs} are matrix elements of the Kohn-Sham and overlap integrals, respectively. These equations can be written more compactly as the coupled matrix equations as

$$\boldsymbol{F}^e\boldsymbol{C}^e = \boldsymbol{S}^e\boldsymbol{C}^e\boldsymbol{\varepsilon}\,, \tag{3.4}$$

$$\boldsymbol{F}^\alpha\boldsymbol{C}^\alpha = \boldsymbol{S}^\alpha\boldsymbol{C}^\alpha\boldsymbol{E}^\alpha\,. \tag{3.5}$$

where $\boldsymbol{C}$ is a $K \times K$ square matrix of the expansion coefficients and $\boldsymbol{\varepsilon}$ ($\boldsymbol{E}$) is a diagonal matrix of the orbital energies for electron (nucleus). Note that the columns of $\boldsymbol{C}$ describes the molecular orbitals. Using the basis, the density of each particle is given by

$$n_e(\boldsymbol{r}) = \sum_i^{occ}\sum_{r,s}^{K} C_{ir}C_{is}{}^* f_r(\boldsymbol{r}) f_s^*(\boldsymbol{r})\,, \tag{3.6}$$

$$n_\alpha(\boldsymbol{r}) = \sum_i^{occ}\sum_{r,s}^{K} C^\alpha_{ir}C^{\alpha\,*}_{is} f_r(\boldsymbol{R}) f_s^*(\boldsymbol{R})\,. \tag{3.7}$$

These equations are solved self-consistently by the same procedure for solving the unrestricted Hartree-Fock (UHF) equations for the electron. The total energy is evaluated as

$$E_{tot} = \sum_i^{occ}\varepsilon_i + \sum_i^{occ}\sum_\alpha E^\alpha_i - \frac{1}{2}(\langle U_{en}\rangle + \langle V^{ee}\rangle + \langle V^{\alpha\beta}\rangle)\,. \tag{3.8}$$

In this treatment, the total energy of the ground state includes so-called the zero point vibrational energy due to the nuclear kinetic energy term.

Each matrix elements in F^e and F^α except for the exchange-correlation potential can be calculated by analytical function $\{f_r\}$ explicitly. On the other hand, It is difficult to calculate the exchange-correlation potential because the fractional powers of the density of particles. I discuss the problem and its prescription in next section.

3.2 Exchange and Correlation potential

The primary computational difficulty in density functional techniques arises from the form of the exchange-correlation potential energy. These involve, at a minimum, fractional powers of the electron density, such as $n^{1/3}$ and $n^{4/3}$. For example, I utilize the X-α approximation for the exchange energy as

$$V_{xc} = 4/3 C_\alpha n^{1/3}\,, \tag{3.9}$$

where

$$C_\alpha = -\left(\frac{9}{4}\alpha\right)\left(\frac{3}{8\pi}\right)^{1/3}\,. \tag{3.10}$$

For all the calculations reported here, I use $\alpha = 0.7$. When the wave function and orbitals are expressed in many-center LCAO expansions as Eq.(3.1), the fractional power of the density does not have a simple closed form as a sum of separate terms. With few exceptions, all of the published LCAO density functional algorithms address this problem by using a three-dimensional grid of points, either to perform the integrations involving the potential by numerical methods, or to fit the potential to a simpler functional form. Because the electron density decreases roughly exponentially away from the nuclear cusps, overlapping atom-centered grids are used almost universally. The alternative is to develop analytical methods that eliminate the grid entirely. Werpetinski and Cook implemented a density functional technique that requires no molecular grid and that includes analytical expressions for the calculations of energy gradients [44]. This method gives smooth energy surfaces in a fraction of the computational time of a grid-based method. The mathematical formalism for this method was originally developed by Dunlap [45].

I start with assuming that the functions $n^{1/3}$ and $n^{2/3}$ are fitted to sets of integrable, atom-centered functions:

$$n^{1/3} \approx \tilde{n}^{1/3} = \sum_i^{Na} a_i A_i \tag{3.11}$$

$$(\tilde{n}^{1/3})^2 \approx \tilde{n}^{2/3} = \sum_i^{Nb} b_i B_i\,, \tag{3.12}$$

where the overbar denotes a fitted approximation to a quantity. In the present implementation, $\{A_i\}$ and $\{B_i\}$ are identical sets of Hermite Gaussian functions, although,

in general, this is not required. Taylor expansions of the exchange energy to first order $n-(\tilde{n}^{1/3})^3$ and $(\tilde{n}^{1/3})^2-\tilde{n}^{2/3}$ give the expression:

$$E_{ex}=\frac{4}{3}C_\alpha\langle\tilde{n}^{1/3}n\rangle-\frac{2}{3}C_\alpha\langle\tilde{n}^{1/3}\tilde{n}^{1/3}\tilde{n}^{2/3}\rangle+\frac{1}{3}C_\alpha\langle\tilde{n}^{2/3}\tilde{n}^{2/3}\rangle\,, \tag{3.13}$$

in which angle brackets indicate integration over all space.

Variational minimization of the exchange energy with respect to the fitting coefficients $\{a_i\}$ and $\{b_i\}$ then gives a set of coupled, nonlinear equations

$$\langle A_i n\rangle-\sum_j^{Na}\sum_k^{Nb}a_jb_k\langle A_iA_jB_k\rangle=0\,, \tag{3.14}$$

$$\sum_{j,k}^{Na}a_ja_k\langle A_jA_kB_i\rangle-\sum_j^{Nb}b_i\langle B_iB_j\rangle=0\,. \tag{3.15}$$

These equations are solved via the Newton-Raphson method to determine the fitting coefficients. Equation (3.14) and (3.15) involve at most three-center integrals, so that this is still an N^3 method. The particular form of Eqs (3.14) and (3.15) depends on the $n^{1/3}$ form for the exchange potential; the addition of correlation corrections or nonlocal exchange-gradient terms would produce a more complicated set of nonlinear equations to solve.

Chapter 4

Results

I use the uncontracted 4-31G basis set for both electron and nucleus multiplying the scale factor ζ_e and ζ_n as

$$\phi_i^\sigma(\boldsymbol{r}) = \sum_r C_{ir}^\sigma\exp[-\zeta_e b_r(\boldsymbol{r}-\boldsymbol{r}_r^C)^2]\,, \tag{4.1}$$

$$\chi_i^{\alpha I}(\boldsymbol{R}) = \sum_r C_{ir}^{\alpha I}\exp[-\zeta_n b_r(\boldsymbol{R}-\boldsymbol{r}_r^C)^2]\,, \tag{4.2}$$

where b_r is an exponent of 4-31G basis set for the hydrogen atom. The scale factors and centers of atom are optimized so that total energy is minimized at the HF level. Table 4.1 is listed the optimized scale factors and distance between two atom centers with mass of particles used in the actual calculation.

Using the variational principle, I determined scaling parameter of exponents for particles, $\zeta_e=0.88651$ and $\zeta_p=35.269$ for H_2 and $\zeta_e=0.78244$ and $\zeta_\mu=2.0912$ for μ_2,

Table 4.1: Mass, optimized exponent and distance between two centers (a.u.).

	Type	Mass	ζ	R
H_2	e	1.0	0.88651	1.4698
	n	1836.0	35.269	
μ_2	e	1.0	0.78244	1.6375
	n	207.0	2.09120	

and also determined the distance between two atom centers(center of Gaussian functions), 1.4698 for H_2 and 1.6375 for μ_2. From these results, I found that exponents for electron are smaller, i.e. molecular orbitals for electron are more broaden, than that of BO($\zeta_e = 1.0$) due to the averaging by nuclear motions. The scale factor for proton is larger, i.e. corresponding molecular orbitals are narrower, than that of muon due to mass. A ratio between main contribution of the exponents for H and for μ is about 18. On the other hand, ratio between mass is about 9(H/μ). The optimized inter atomic distance of H_2 is shorter than that of μ_2 because of the difference of their mass, meaning that μ_2 is loosely bound than H_2.

Density for the electron and the nucleus along the z-axis are defined as

$$\begin{aligned} n_e(z) &= \sum \int dx \int dy n_e^\sigma(\boldsymbol{r}) \,, \\ n_\alpha(Z) &= \sum \int dX \int dY n_\alpha^I(\boldsymbol{R}) \,. \end{aligned} \tag{4.3}$$

The difference of density is also defined as

$$\Delta n_{e(or\ n)}(z) = n^{H_2}_{e(or\ n)}(z) - n^{\mu_2}_{e(or\ n)}(z) \tag{4.4}$$

where e and n denote electron and nucleus, respectively. The density of particles in Eq.(4.3) and its difference in Eq.(4.4) between H_2 with μ_2 along the z-axis are depicted in Figs. 4.1-(a) and -(b), respectively. The electronic density of H_2 has difference from that of μ_2 mainly classified under two regions. I divide the difference of electronic density Δn_e into two regions, (i-a) inside region of two peaks of density of proton(about $z = \pm 0.735$) and (ii-a) outside region of two peaks of density of proton. In (i-a), the electron density difference is positive. On the other hand, in (ii-a), the electron density difference is negative. These results are due to the delocalization of density of the muon(see Fig. 4.1-(b)). The density of the proton is localized at atom centers in comparison with density of muon, which is delocalized as the electron, as expected by results from Table 4.1. The difference of the nuclear density Δn_n is mainly classified under three regions, (i-b) center of whole system, (ii-b) inside region of atom centers of the proton, and (iii-b) outside region of the atom centers. In (i-b), the difference is negative due to the non-negligible overlap of wavefunctions for the muon. On the other hand, wavefunctions for proton

have little overlap. In (ii-b), the difference is positive, because the density of the proton is localized at the atom centers owing to heavy mass. In (iii-b), the difference is negative due to the delocalization of the density of muon. These indicate that the proton is less mobile than the muon from the centers of subsystem. Table 4.2 shows the energy of

Table 4.2: Total energy (a.u.) obtained by several methods.

	HF	LDA	Static GWA	CI	Exact
NBO H_2	-1.04638372	-1.00843168	-1.07825734	-1.06758843	-1.1744746[a]
NBO μ_2	-0.92061958	-0.88714924	-0.93751595	-0.94157746	

[a] [46] : Kolos et al. obtained by Hylleraas type wavefunction at r_e=1.401 a.u.

the individual motion obtained from several methods. The energy obtained by the HF method is lower than that by the LSD, because, in general, the LSD does not contain the self-interaction correction(SIC) in contrast with the HF method. From these results, I found that results obtained by the static GWA are improved compared with those by the HF or the LSD and, however, the result for H_2 is lower than that by the CI because of the effects of decoupling, the choice of static limit, and so on. Then, I conclude that the GWA works well to the molecules in the framework of the NBO DFT theory rather than the LSD or HF, though the correlation effects are too much overestimated.

Table 4.3: HOMO-LUMO orbital energy gap for electron obtained by several methods(a.u.).

	HF	LDA	Static GWA
$\Delta E_{HOMO-LUMO}$ for H_2	-0.77728993	-0.31131811	-0.72868981
$\Delta E_{HOMO-LUMO}$ for μ_2	-0.69213000	-0.26489982	-0.64642737

Table 4.3 shows the orbital energy gap between HOMO and LUMO(HOMO-LUMO gap) $\Delta E_{HOMO-LUMO} = \varepsilon_{HOMO} - \varepsilon_{LUMO}$ for the electron obtained from the HF, LSD, and GWA. As it is likely to be much underestimated for the HOMO-LUMO gap by

the LSD for lack of the SIC and to be overestimated by the HF because of shortage of correlation effects, although the HF contains the effect of the SIC. The results by the GWA are much improved with respect to the LSD and are lower than those by the HF, meaning that the gap is improved by the GWA.

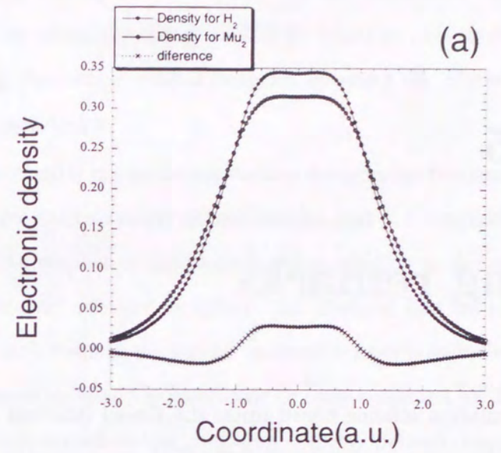

Figure 4.1: Plot of particle density of H_2 and μ_2 and its difference along z-axis. (a) Electronic density. (b) Nuclear density. Density difference is defined as $n^{H_2}_{e(orn)} - n^{\mu_2}_{e(orn)}$. In figures, Mu means μ.

Chapter 5

Concluding remarks

A NBO-DFT calculation scheme based upon the Green function techniques is presented to apply molecular systems. I generalize the GW approximation to treat a molecular system consists of the mixture of electron and fermion nuclei and depict diagrams appearing in the expansion of the GWA. A numerical calculation for *individual* motion of simple systems such as hydrogen molecule and muon molecule is attempted by means of the Gaussian basis sets. Using the variational principle, I determined scaling parameter of exponents for particles and the distance between two atom centers. From these results, I found that exponents for electron are smaller, i.e. molecular orbitals for electron are more broaden, than that of BO($\zeta_e = 1$) due to the averaging by nuclear motions. I also found that the optimized inter atomic distance of H_2 is shorter than that of μ_2 because of the difference of their mass, meaning that muon molecule is loosely bound than hydrogen molecule. I depicted density of particles in Fig. 2.1. I found that density of proton is much less broaden than that of muon and that wavefunctions for muon have non-negligible overlap. I evaluate the total energy of *individual* motion of those molecules and orbital energy gap between HOMO and LUMO for the electron at several approximation levels. From these results, I found that results obtained by the static GWA are improved compared with those by the HF or the LSD. Then, I conclude that the GWA works well to the NBO treatment of molecular theory.

The results obtained from the method are far from in such small systems because of the lack of cusp in the basis used here. This feature may not be essential for the

physical properties, because the cusp condition is improved by using the Slater type function. Although Totsuji et al. carried out self-consistent calculation of the proton tunneling system by using the Slater orbital for electron and proton at zero temperature [47], to evaluating the atomic orbital integrals by using the Slater type function are very expensive in the calculation.

The present method is useful for crystalline systems for two reasons. First, in the crystalline system, there exist so many normal modes that it is tractable to calculate averaged electronic state with respect to the motion corresponding to the normal mode. Although an approach of present method is direct, the method has an information of averaged electronic states with respect to nuclear motion(density), so-called zero point vibration. In particular, I consider that the electronic density obtained by X-ray experiment[48] of $KD_3(SO_4)_2$ may correspond to the averaged density. Second, the present method can be extended to framework within the finite temperature based upon the Matsubara Green function method [33]. This extension may enable us to investigate the phase transition of the systems mentioned at the introduction.

Let us consider the transition properties of KH_2PO_4 (KDP) type crystals. In these compounds, large isotope effect on the transition temperature is found. For example, the transition temperature of phase transition increases by deuteration as listed in Table 5.1.The ratio of T_c^H to T_c^D is about 1.5$\sim$1.7. As other examples, there exists deuteration-induced phase transition found in $M_3H(XO_4)_2$ (M=K, Rb, Cs and X=S, Se) type crystals, derivatives of 9-hydroxyphenalenone, and $(NH_4)_2MCl_6$ (M=Sb, Pb, Pt, Te, Se) type crystals. There are few materials with such a large isotope effect on the transition temperature except for these hydrogen-bonded materials.

To explain the mechanism of the phase transition of these hydrogen-bonded (anti-) ferroelectronic materials, two different approaches have been proposed. One is the proton tunneling model, which is classified as a dynamical effect. The model tells that the mechanism is owing to a quantum effect of the proton (deuteron) transferring between two equilibrium positions, i.e. the quantum tunneling. Because lighter mass nuclei experience the effect more strongly, T_c of protonated compounds decreases due to the tunneling of protons disturbing a long-range order associated with a static position of the protons.

Table 5.1: Several compounds with large isotope effect on the transition temperature by deuteration and their transition temperature.

Compounds	T_c^H (K)	$T_c^D(K)$	T_c^D/T_c^H
KH_2PO_4	123	213	1.7
RbH_2PO_4	146	218	1.5
$NH_4H_2PO_4$	147	242	1.6
CsH_2PO_4	153	267	1.7

The tunneling behavior has not been elucidated by experiments. Recently, Matsuo et al. observed an indication of the proton tunneling in 5-bromo-9-hydroxyphenalenone [49]. The other concerns with an empirical correlation between transition temperature and a discrepancy of O-O distances between a protonated compound and a deuterated one, where the former is shorter than the later in general. The discrepancy is called the geometrical isotope effect, usually called as Ubbelohde effect, which is classified a static effect. These two model are, however, contrary to each other, because a potential for the proton is identical with that for the deuteron in tunneling model.

By using the present method, these two different models can be comprehended systematically as follows: First, the dynamical tunneling of proton may be interpreted by dynamics of the nuclear wavefunctions localized at two energy minima. The ground state and first excited state are the linear combination of the nuclear wavefunctions localized at two minima and energy level of the localized states split into two levels. the time-dependent probablity amplitude obtained by the nuclear wavefunction. The tunneling occurs when the energy level of the two energy minima and/or the energy level of thermally activated states at minimum and the ground state localized at anther minimum are consistent with each other. The former is classified by the resonant tunneling and the later the thermally activated tunneling. Under the NBO point of view, these tunneling energy levels can be calculated directly including the effect of all the other particles and a potential energy surface along unknown reaction paths should not be needed. Using

Table 5.2: Inter particle distance of H_2 and HD (Å)

	H_2	HD
n-n ([29])	0.7964	0.7859
n-n (Exptl.)	0.74677(10)	0.74604(10)
e-e	1.042	1.034

quantum dynamics under the NBO regime can perform the tunneling dynamics. Second, the geometrical isotope effect is as a result of the expectation values of positions of particles including the effect of vibrational motion. At lower temperature, the zero point vibration mainly dominates the effect. In the present method, the quantum effect of the nuclei, especially the zero point vibration, is included. In the previous work, I have evaluated the inter-nuclear distance of the hydrogen molecule and its isotopomers as shown in Table 5.2. From the result, the expectation values of inter-nuclear distances of H_2 and HD are different from each other due to the difference of mass. Tendency of the inter-nuclear distances is H_2 >HD. Although the absolute values are worse in comparison with the experimental data, their behavior is accord with that of the experimental data. This behavior is expected to O-H and O-D bonds, i.e. O-H>O-D, which is responsible for the discrepancy of the O-O distance af following mechanism: Because the zero-point motion, electronic density on the deuteron has more localized behavior than that on the proton, the electron on the proton more strongly interact with the electrons on the hydrogen-bonded oxygen atom than the electron on the deuteron does. Then the proton with a bonded oxygen is attracted toward the hydrogen-bonded oxygen by this effect because of weak chemical bond between the proton and the hydrogen-bonded oxygen. In order to calculate the transition temperature, I need to proceed the method by using temperature Green function method or the centroid molecular dynamics method discussed in the final part. I will cope with the difficult problems in future.

Part II

Theoretical studies on anomalous phases of proton and electron coupled systems

Chapter 1

Introduction

Finding novel and unique functionality by means of organic molecules is one of the most attractive problems in the physical chemistry. So far a lot of models for functional molecules have been suggested and proposed in view of molecular technology. However, there are many problems to make the functionality realized at macroscopic size. If one makes the molecular assembled systems by constructing the molecules with the functionality, the designed functionality may vanish at macroscopic size. Moreover, in general, it has been known that a formation of assembly of the organic molecules is anisotropic and there is an intrinsic instability in such low dimensional systems. In the molecular assembled systems, inter-molecule interactions play the important role in the formation. Characters of each molecule are varied by the inter-molecule interaction and the systems exhibit new characters correspond to the formation of assembly. Therefore, when I find new functionality, the key point is to predict cooperative effects between the characters of each molecule and a field generated by the assemblies.

The cooperative proton and electron transfer (PET) reactions have been attracted much attention from theoretical and experimental point of view. One of such systems, there exists in a DNA double strand [50]-[52]. They may give a critical information on cooperative effect between the electron and the proton. Structure of DNA is shown in Fig. 1.1. The structure is a one-dimensional spiral chain consists of two chains around a central axis. These two chains are stabilized by two base pairs (A and T, C and G). It is well known that an arrangement of these pairs determines a certain genetic information.

These pairs have two or three hydrogen-bonded interactions. Each acid is electron donor or acceptor corresponding to its ionicity. The hydrogen bonds are also strongly affected from the ionicity of the bases.

One of the most simplest PET systems, there exists quinhydrone crystal [53]. The quinhydrone which consists of quinone (electron acceptor) and p-hydroquinone (electron donor) is one of the charge transfer complexes. The crystalline quinhydrone is an insulator at atmospheric pressure. The quinhydrone and its derivatives may be four different charge transfer states (see Fig. 1.2): (a) a normal state, (b) an electron transfer (ET) state, (c) a proton transfer (PT) state, and (d) a combination of ET and PT, so-called the PET state. These states can exhibit different conductivity because the ET and PT states are ionic and the PET state is characterized by hydrogen-bonded neutral radical. At the high pressure, Mitani et al. observed vibrational spectra of CO and OH bonds depicted in Fig. 1.3 and found the indication of PET state [54].

History of studying conductivity and superconductivity of organic materials is shorter than that of inorganic materials. Because the first observation of conductivity and superconductivity in an organic material were reported in 1973 and in 1980, respectively. Following this, many organic (super-) conductors have been synthesized. The highest transition temperature of the organic superconductors is almost 11K, which is, however, about one fifteenth of the highest inorganic one. Synthesizing a novel material with the higher transition temperature is one of important topics in this area. These compounds mainly consist of a combination of the charge transfer complexes, in which an intermolecular charge transfer, which is essential to the conductivity, occurs. Organic molecular crystals are different from the inorganic ones in their constituent elements. The former consists of molecules and the later consists of one atom or plural atoms. Then the factors dominating their physical properties of the organic ones are properties of the constituent molecules, combinations of molecules, intermolecular distance, and orientation of the molecules. Tuning the factors can easily control the properties On the other hand, the factors of the inorganic one are the combinations of atoms or impurities. It is relatively difficult to predict their properties at the present time.

In usual metallic materials, one can consider that conduction electrons freely move

in an averaged single particle potential and can predict their conductivity by means of the band theory based on the single-particle picture. However, there exist materials exhibiting a different nature with respect to the usual metals. Some materials, which are predicted exhibiting metallic property and indeed show metallic conductivity at a certain temperature and higher, becomes the insulator at lower temperature. One of the typical phenomena is the charge density wave (CDW) or the spin density wave (SDW). The CDW and SDW states have spatial periodicity, which are in general longer than lattice constants, of electron charge density and spin density, respectively. Many-body effects, say the electron-phonon interaction or the electron correlation, causes them. The schematic diagram of the CDW in a one-dimensional chain, which consists of identical atoms, is depicted in Fig. 1.4. Fig. 1.4-(a) and Fig. 1.4-(b) denote a normal (metallic) state and a CDW state with the periodic length $2a$, where a denotes a lattice constant. The CDW is due to the dimerization of the two atoms as shown in Fig. 1.4-(b) causing band gap around $k = \pi/2a$. This phase transition is also called as the Peierls transition and usually follows with distortion of lattices. The schematic diagram of the SDW also is shown in Fig. 1.5. (a), (b), (c), (d) represent paramagnetic, antiferromagnetic, spin Peierls, delocalized antiferromagnetic cases, respectively. At high temperature, spins on the atoms turn to random orientations. As temperature decreases, the spins are arranged to bring about order due to the magnetic interaction between atoms shown in (b). Dimerization of two spins, whose combined spin is zero, is responsible for the spin Peierls transition as an analogy of the CDW depicted in (c). As the case of (d), densities of up and down spin wave with a periodicity and the whole system is weak antiferromagnetic. Comparison with (b), magnitude of spins on each atom is smaller and consequently total energy of the state is lower than (b). The SDW states do not follow with distortion of lattices as is often the case of the CDW. The SDW is collective excitation associated with magnetism and occurs in both ferromagnetic and antiferromagnetic systems.

In this part, I investigate transition properties of a model PET system by using the band theory. In chapter 2, I explain a theoretical background of calculation of transition temperature of singly ordered phases as the singlet superconductivity (SSC), SDW, and CDW in terms of the temperature Green function method. Especially, I

apply an approximation method known as g-model to this problem [55]-[56]. Chapter 3 concerns with numerical results of the energy band and transition temperature of anomalous phases in the pseudo one-dimensional quinhydrone crystal. I consider the two model cases: unit cell consists of (1) benzoquinone and *p*-hydroxyquinone and (2) of two semiquinones forming a pseudo one-dimensional chain. A possible mechanism of appearing these anomalous phases is discussed in relation to the PET reaction and applied field. Chapter 4 concerns concluding remarks.

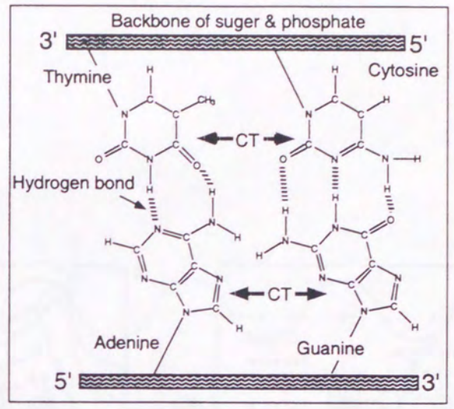

Figure 1.1: Hydrogen bond network in the DNA double strand.

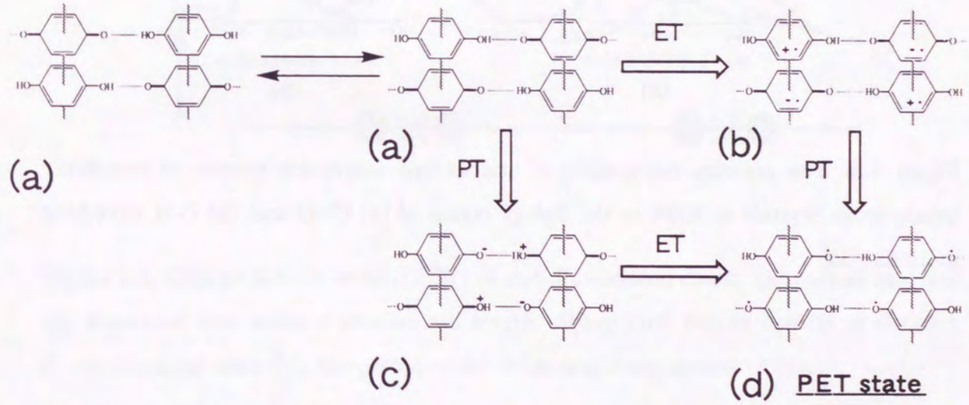

Figure 1.2: Schematic diagram of the PET reaction path. There exist two different paths of transition from normal state to proton and electron transfer(PET) state.

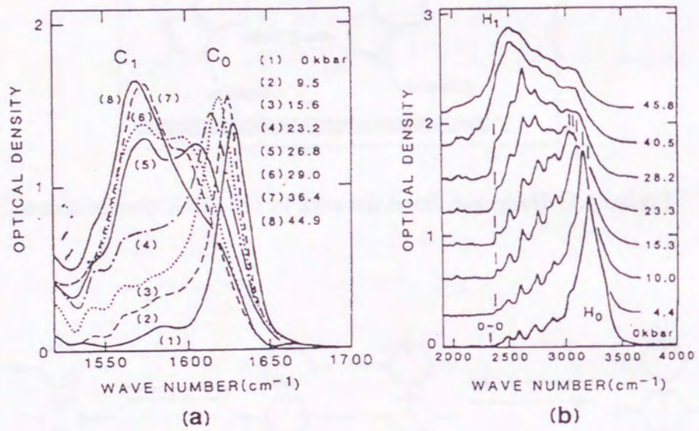

Figure 1.3: The pressure dependence of unpolarized absorption spectra of monotonic quinhydrone crystals at 300K in the energy region of (a) C=O and (b) O-H stretching motions. [54]

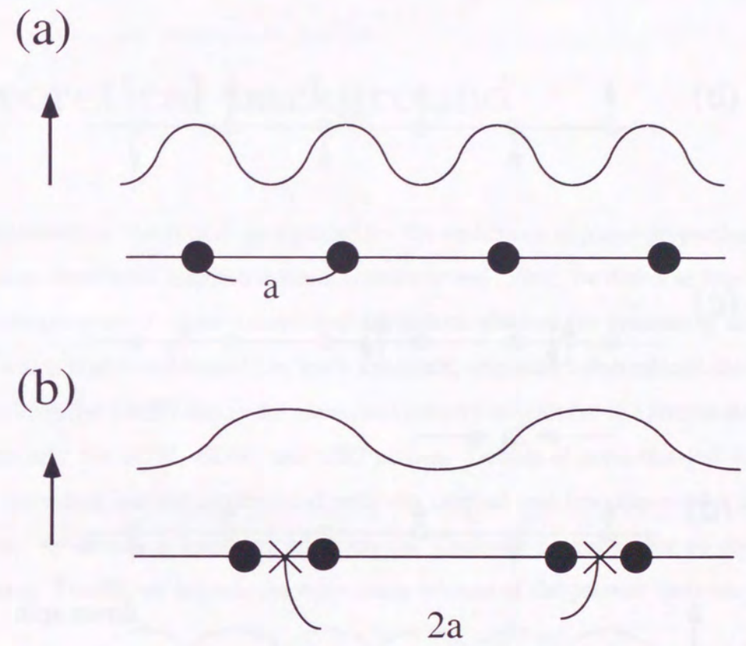

Figure 1.4: Charge density wave (CDW) in one-dimensional chain: (a) normal case and (b) dimerized case where a denotes cell length. Wavy lines denote density of electron. Comparison (a) with (b), the period of (b) is twice as long as that of (a).

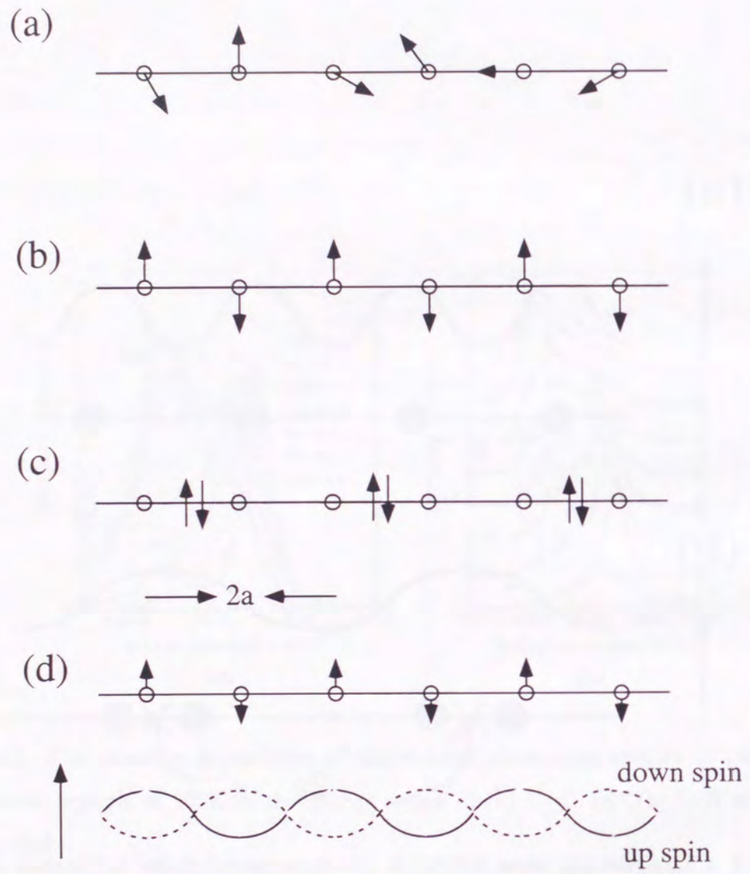

Figure 1.5: Spin density wave (CDW) in one-dimensional chain: (a) ferromagnetic case, (b) antiferromagnetic case, (c) dimerized spin case, and (d) delocalized antiferromagnetic case, where a denotes cell length. A wavy line and doted wavy line in (d) denote up and down spin density of electron. Comparison (a) with (c) and (d), the period of (c) and (d) are twice as long as that of (a).

Chapter 2

Theoretical background

In this section, theoretical background for the evaluation of phase properties based on the temperature Green function method is summarized. First, we derive an expression for critical temperature of phase transition of anomalous phase in the systems by using the g-model, which is an extension of Gor'kov's approach, originally reformulated the Bardeen-Cooper-Schrieffer (BCS) theory for superconductivity in terms of the temperature Green function, into the SDW, CDW, and SSC phases. Details of mathematical foundation on the derivation are almost identical with the original one (see appendices 2-3 and 2-4). Next, we discuss a screening effect on the Coulomb potential due to the electron correlation. Finally, we explain the calculation scheme of the present method.

2.1 g-model

I investigate anomalous phases of coupled system of electron and proton by means of the approach by Kimura et al [55]. Before I discuss the condensed phase of the system, it is instructive to summarize the single-particle states of the system. Here, I arrange the electron-electron interaction in a manner which is known as g-model and derive the expression of transition temperature T_c. The interaction Hamiltonian is given as

$$H_{int} = \frac{1}{4} \sum_{ijkl} \sum_{\alpha\beta\gamma\delta} \Gamma_{ijkl}^{\alpha\beta\gamma\delta} a_{i\alpha}^{\dagger} a_{j\beta}^{\dagger} a_{k\gamma} a_{l\delta} \,, \tag{2.1}$$

where the vertex function and matrix element of interaction are defined as

$$\Gamma_{ijkl}^{\alpha\beta\gamma\delta} = \langle i_\alpha j_\beta | k_\gamma l_\delta \rangle \delta_{\alpha\delta}\delta_{\beta\gamma} - \langle i_\alpha j_\beta | l_\delta k_\gamma \rangle \delta_{\alpha\gamma}\delta_{\beta\delta} \ , \tag{2.2}$$

$$\langle i_\alpha j_\beta | k_\beta l_\alpha \rangle = \int\int d\boldsymbol{r}_1 d\boldsymbol{r}_2 \phi_{i\alpha}^*(\boldsymbol{r}_1)\phi_{j\beta}^*(\boldsymbol{r}_2)V(\boldsymbol{r}_1,\boldsymbol{r}_2)\phi_{k\beta}(\boldsymbol{r}_2)\phi_{l\alpha}(\boldsymbol{r}_1) \ , \tag{2.3}$$

$\phi_{i\alpha}$ means a wavefunction of an i-th level with a spin α. I here restrict ourselves to take account of only the lowest conduction c and the highest valence v bands. A role of the other bands which lie far from the Fermi surface is to screen the interaction of v and c bands. Thus, Eq.(2.1) is reduced to

$$\begin{aligned}\tilde{H}_{int} = \frac{1}{4}\sum_{k_1k_2k_3k_4}\delta(k_1+k_2+k_3+k_4)\sum_{\alpha\beta\gamma\delta} \\ \Big[\tilde{\Gamma}_{vvvv}^{\alpha\beta\gamma\delta}a_{vk_1\alpha}^\dagger a_{vk_2\beta}^\dagger a_{vk_3\gamma}a_{vk_4\delta} + \tilde{\Gamma}_{vvcc}^{\alpha\beta\gamma\delta}a_{vk_1\alpha}^\dagger a_{vk_2\beta}^\dagger a_{ck_3\gamma}a_{ck_4\delta} + \\ 2\tilde{\Gamma}_{vcvc}^{\alpha\beta\gamma\delta}a_{vk_1\alpha}^\dagger a_{ck_2\beta}^\dagger a_{vk_3\gamma}a_{ck_4\delta} + (v\leftrightarrow c)\Big] \ ,\end{aligned} \tag{2.4}$$

where $\tilde{\Gamma}$ is a screened vertex part. In the following analysis, I parameterize the matrix elements of the interaction by the values evaluated at the Fermi momentum Then the coupling constants are approximated a

$$\tilde{\Gamma}_{vvvv}^{\alpha\beta\gamma\delta} = \tilde{\Gamma}_{vvvv}^{\alpha\beta\gamma\delta} = g_1(\delta_{\alpha\delta}\delta_{\beta\gamma} - \delta_{\alpha\gamma}\delta_{\beta\delta}) \ , \tag{2.5}$$

$$\tilde{\Gamma}_{vvcc}^{\alpha\beta\gamma\delta} = \tilde{\Gamma}_{ccvv}^{\alpha\beta\gamma\delta} = g_2(\delta_{\alpha\delta}\delta_{\beta\gamma} - \delta_{\alpha\gamma}\delta_{\beta\delta}) \ , \tag{2.6}$$

$$\tilde{\Gamma}_{vcvc}^{\alpha\beta\gamma\delta} = \tilde{\Gamma}_{cvcv}^{\alpha\beta\gamma\delta} = g_3\delta_{\alpha\delta}\delta_{\beta\gamma} - g_4\delta_{\alpha\gamma}\delta_{\beta\delta} \ , \tag{2.7}$$

where they are evaluated from the screened interaction at Fermi momentum which is mentioned in section 2.2.

Now I define the order parameters, which are helpful to construct the mean field Hamiltonian, as defined as

$$2\tilde{\Delta}_1 = \sum_{\boldsymbol{k}\alpha}\langle a_{v\boldsymbol{k}\alpha}^\dagger a_{c\boldsymbol{k}\alpha}\rangle = \sum_{\boldsymbol{k}\alpha}\langle a_{c\boldsymbol{k}\alpha}^\dagger a_{v\boldsymbol{k}\alpha}\rangle \ , \tag{2.8}$$

$$2\tilde{\Delta}_2 = \sum_{\boldsymbol{k}\alpha}\alpha\langle a_{v\boldsymbol{k}\alpha}^\dagger a_{c\boldsymbol{k}\alpha}\rangle = \sum_{\boldsymbol{k}\alpha}\alpha\langle a_{c\boldsymbol{k}\alpha}^\dagger a_{v\boldsymbol{k}\alpha}\rangle \ , \tag{2.9}$$

$$2\tilde{\Delta}_3 = \sum_{\boldsymbol{k}}\langle a_{v\boldsymbol{k}\uparrow}^\dagger a_{v-\boldsymbol{k}\downarrow}^\dagger\rangle = \sum_{\boldsymbol{k}}\langle a_{v-\boldsymbol{k}\downarrow}^\dagger a_{v\boldsymbol{k}\uparrow}^\dagger\rangle \ , \tag{2.10}$$

for the singlet exciton, triplet exciton, and singlet Cooper pair, respectively. $\alpha = \pm$ for the spin up and down. Thus, I can derive a mean field Hamiltonian from Eqs.(2.8)-(2.10) as

$$\begin{aligned}H_{\rm int}^{\rm MF} = -\sum_{\boldsymbol{k}\alpha}\Delta_1\left(a_{v\boldsymbol{k}\alpha}^\dagger a_{c\boldsymbol{k}\alpha} + a_{c\boldsymbol{k}\alpha}^\dagger a_{v\boldsymbol{k}\alpha}\right) + \sum_{\boldsymbol{k}\alpha}\alpha\Delta_2\left(a_{v\boldsymbol{k}\alpha}^\dagger a_{c\boldsymbol{k}\alpha} + a_{c\boldsymbol{k}\alpha}^\dagger a_{v\boldsymbol{k}\alpha}\right) \\ -\sum_{\boldsymbol{k}}\Delta_3\left[a_{i\boldsymbol{k}\uparrow}^\dagger a_{i-\boldsymbol{k}\downarrow}^\dagger + a_{i-\boldsymbol{k}\downarrow}a_{i\boldsymbol{k}\uparrow} + (v\leftrightarrow c)\right]\end{aligned} \tag{2.11}$$

where

$$\lambda_1 = -g_2 - 2g_3 + g_4 \tag{2.12}$$

$$\lambda_2 = g_2 + g_4 \tag{2.13}$$

$$\lambda_3 = -(g_1 + g_2) \tag{2.14}$$

and

$$\Delta_x = \lambda_x\tilde{\Delta}_x \ , \quad x = 1,2,3 \ , \tag{2.15}$$

The total Hamiltonian with the mean field approximation is given as

$$H = H_0 + H_{\rm int}^{\rm MF} \ . \tag{2.16}$$

Let us define the following Green functions to characterize the CDW, SDW, and SSC phases as

$$G_\alpha^v(\boldsymbol{k},t) = -\langle {\rm T}[a_{v\boldsymbol{k}\alpha}(t)a_{v\boldsymbol{k}\alpha}^\dagger(0)]\rangle \ , \tag{2.17}$$

$$F_\alpha^{cv}(\boldsymbol{k},t) = -\langle {\rm T}[a_{c\boldsymbol{k}\alpha}(t)a_{v\boldsymbol{k}\alpha}^\dagger(0)]\rangle \ , \tag{2.18}$$

$$\tilde{F}_{\alpha\beta}^v(\boldsymbol{k},t) = -\langle {\rm T}[a_{v-\boldsymbol{k}\alpha}^\dagger(t)a_{v\boldsymbol{k}\beta}^\dagger(0)]\rangle \ . \tag{2.19}$$

In addition, there is another set that is obtained by interchanging v and c.

From the equation of motion within the mean field approximation or by the decoupling procedure to the equation of motion for the Green function, I obtain equations for the Green function, which are separated into two parts for up and down spins. Then, obtain

$$\begin{pmatrix} G_\alpha^v(\boldsymbol{k},\omega_n) \\ F_\alpha^{cv}(\boldsymbol{k},\omega_n) \\ \tilde{F}_{-\alpha\alpha}^v(\boldsymbol{k},\omega_n)\end{pmatrix} = \frac{1}{\omega_n^2 + \tilde{\epsilon}_\alpha(\boldsymbol{k})^2}\begin{pmatrix} -(i\omega_n - \epsilon_\alpha(\boldsymbol{k})) \\ \Delta_1 + \Delta_2 \\ \alpha\Delta_3\end{pmatrix} \ , \tag{2.20}$$

where

$$\tilde{\epsilon}_\alpha(\boldsymbol{k})^2 = \epsilon(\boldsymbol{k})^2 - \Delta_\alpha^2 \ , \tag{2.21}$$

$$\Delta_\alpha^2 = (\Delta_1 + \alpha\Delta_2)^2 + \Delta_3^2 \ , \tag{2.22}$$

and $\alpha = \pm 1$ is for the spin up and down, respectively.

For the simplicity, in Eq.(2.20) I suppose a symmetry ($\tilde{\epsilon}^j(\boldsymbol{k}) = -\tilde{\epsilon}^i(\boldsymbol{k})$, $\tilde{\epsilon}^i(-\boldsymbol{k}) = \tilde{\epsilon}^i(\boldsymbol{k})$) hereafter. I turn to the solution for the order parameter Δ_1. From Eqs.(2.8)-(2.10) and (2.17)-(2.19), I obtain

$$\Delta_1 = \frac{\lambda_1}{2}\sum_{\boldsymbol{k}\alpha} F_\alpha^{cv}(\boldsymbol{k}, t=0) = \frac{\lambda_1}{2} T \sum_{\boldsymbol{k},\omega_n,\alpha} F_\alpha^{cv}(\boldsymbol{k},\omega_n) \ . \tag{2.23}$$

Inserting Eq.(2.20) into the above, I get a set of self-consistent equation:

$$\Delta_1 = \frac{\lambda_1}{4}\left[(\Delta_1+\Delta_2)\sum_{\boldsymbol{k}}\frac{1}{\tilde{\epsilon}_{\boldsymbol{k}\uparrow}}\tanh\frac{\tilde{\epsilon}_{\boldsymbol{k}\uparrow}}{2T} + (\Delta_1-\Delta_2)\sum_{\boldsymbol{k}}\frac{1}{\tilde{\epsilon}_{\boldsymbol{k}\downarrow}}\tanh\frac{\tilde{\epsilon}_{\boldsymbol{k}\downarrow}}{2T}\right] \ . \tag{2.24}$$

In a similar way, I obtain for Δ_2 and Δ_3,

$$\Delta_2 = \frac{\lambda_2}{4}\left[(\Delta_1+\Delta_2)\sum_{\boldsymbol{k}}\frac{1}{\tilde{\epsilon}_{\boldsymbol{k}\uparrow}}\tanh\frac{\tilde{\epsilon}_{\boldsymbol{k}\uparrow}}{2T} - (\Delta_1-\Delta_2)\sum_{\boldsymbol{k}}\frac{1}{\tilde{\epsilon}_{\boldsymbol{k}\downarrow}}\tanh\frac{\tilde{\epsilon}_{\boldsymbol{k}\downarrow}}{2T}\right] \ , \tag{2.25}$$

$$\Delta_3 = \frac{\lambda_3}{2}\Delta_3\sum_{\boldsymbol{k}}\frac{1}{\tilde{\epsilon}_{\boldsymbol{k}}}\tanh\frac{\tilde{\epsilon}_{\boldsymbol{k}}}{2T} \tag{2.26}$$

According to the procedure[57], I also suppose that the parameters of g in Eqs.(2.5)-(2.7) is constant in the energy region ending at the cut-off value $-E_c$. Physically E_c must be determined by the energy at which the velocity of the holes becomes so large that during than the correlation length. I designated also $\mu = -\zeta$ ($\zeta > 0$). Here, it is supposed that the top energy of the higher band (v band) with the width $E_{\rm w}^v$ is $-E_v$ and the top energy of the lower band (c band) is $-E_c$. I consider the case when $E_v = 0$.

For $\zeta < E_c$ the transition temperatures of various singly ordered phases is given by

$$T_c^{\rm phase} = \begin{cases} 1.13\left[\zeta\left(E_c-\zeta\right)\right]^{1/2} e^{-\frac{1}{K_{\rm phase}}} & , \quad K_{\rm phase} > 0 \\ 0 & , \quad K_{\rm phase} \le 0 \end{cases} \ , \tag{2.27}$$

where

$$K_{\rm phase} = \begin{cases} \lambda_1\rho_v & , \text{for CDW} \\ \lambda_2\rho_v & , \text{for SDW} \\ \lambda_3\rho_v & , \text{for SSC} \end{cases} \ . \tag{2.28}$$

ρ_i corresponds to the density of states for the cylindrical isoenergetic surface for v band.

2.2 Screening effects

The screening effect for the electron-electron interaction is treated by the perturbation method. The effective interaction is written in k space as

$$W(k) = \left[1 - u(k)\Pi(k)\right]^{-1} u(k) \ . \tag{2.29}$$

where W and u are the effective and bare potentials, respectively. I employ the random phase approximation (RPA) for the proper polarization part, Π, which is given by the ring diagram in Fig. 2.1 and denoted by Π^0, it follows that

$$\Pi_{sr}^0(k,\omega) = \frac{4}{V}\sum_q\sum_b^{un}\sum_{b'}^{occ}\frac{\langle s|b,k+q\rangle\langle b,k+q|r\rangle\langle r|b',q\rangle\langle b',q|s\rangle}{\omega - \epsilon_b(k+q) + \epsilon_{b'}(q)} \ . \tag{2.30}$$

I make a small cut-off around the fermi momentum in carrying out the summation with respect to q, because electrons in this small region are responsible for the instabilities associated with phase transitions. I use the cutoff energy $E_{\rm cut} = 0.098$ (eV). In order to improve the RPA for the polarization part, I take into account the oyster diagram. I am obliged to use an approximation in which the bare electron-electron interaction is restricted only to the one-center type. Thus I have

$$\Pi_{sr}^1(k) = -\frac{1}{2}\sum_t \Pi_{st}^0(k) w_{tt}(k) \Pi_{tr}^0(k) \ . \tag{2.31}$$

For the bare potential $u_{rs}(n)$(eV), I adopt the Ohno potential[58]:

$$u_{rs}(n) = \frac{14.40}{\sqrt{R_{rs}(n)^2 + 51.8328(1/F_r + 1/F_s)^2}} \ , \tag{2.32}$$

where $R_{rs}(n)$ is the distance from the r-th site of the 0-th cell to the s-th site of n-th cell (in the unit of A) and F_r is a constant value for atom at site r listed in Table 2.1. Because

Table 2.1: Parameter appearing in the Ohno potential

	C	O	H
F(atom)	11.089	13.599	12.845

the Dyson equation for the effective potential is an integral equation in the coordinate space and is difficult to solve, I take the Fourier transform of $W_{rs}(n)$ and its inverse as

$$W_{rs}(n) = \frac{1}{L}\sum_{k} e^{ikn} w_{rs}(k) \tag{2.33}$$

$$W_{rs}(k) = \sum_{n=-N}^{N} e^{-ikn} w_{rs}(n) \ . \tag{2.34}$$

Once the screened Coulomb potential W is calculated, T_c can be evaluated substituting them into Eqs.(2.5)-(2.7) instead of the bare Coulomb potential V Eq.(2.3).

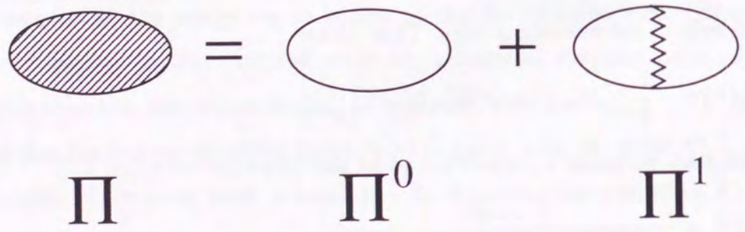

Figure 2.1: Fynman diagrams of the polarization part considered in this work.

Chapter 3

Numerical results

A model system is given in Fig. 3.1. I construct two models as follows: (i) the molecule A is a *p*-hydroquinone and the molecule B is a benzoquinone and (ii) both the molecule A and B are semiquinones. Molecular structures for the *p*-hydroquinone and the benzoquinone used here are experimental values for the case of triclinic crystal obtained by Sakurai [59]. On the other hand, that for the semiquinone used here is an optimized structure obtained by the ab initio calculation. I assume that the structure of the monomers does not change by the displacement Δx, which denotes distance form a center of molecule A to a right overhead center of molecule B and vertical separation R also depicted in Fig. 3.1.

I performed band structure calculations of the model systems within the tight-binding approximation, where I use an extend Hückel program package [60]. Figs. 3.2 list the averaged energy of the model systems for various values of Δx and R obtained by assuming two-dimensional periodicity. Note that the experimental values are nearly $\Delta x = 2.25$ (Å) and R =3.25. The average energies of both model (i) and (ii) have minimum at $\Delta x = 2.5$. These results tell that the model (i) is more stable than the (ii) in energetically. I found that the model (ii) has metastable state at $\Delta x = 0$ and the model (i) does not. Figs. 3.3 depicts the highest valence (v) and the lowest conduction (c) band structures of model (i) and (ii) at $R = 3.25$ Å. From these figures, I found that the model (i) is an insulator for each Δx and R, because there exists a band gap between v and c bands. I found that these situation does not change by tuning the vertical separation at least R =2.75

Å. On the other hand, the model (ii) has a metallic character, because the energies of v and c band at the Fermi momentum k_F are degenerate. With decreasing the vertical separation, it appears the two-band character. In general, the energy gap between c and v bands at k_F is increased by the electron correlation effect so that model (i) is still a insulator and model (ii) may be the insulator or metal after taking into account of the electron correlation.

In order to clarify their conductivity, I next evaluate the λ's of CDW, SDW, SSC phases only for the model (ii). I found that $\lambda_{CDW} < 0$, $\lambda_{SDW} > 0$, and $\lambda_{SSC} < 0$ for each case and then the system exhibits the SDW insulator. Fig. 3.5 shows critical temperature of the SDW phase at various R and Δx values. This result tell me that when $\Delta x = 0$, i.e. the molecule A is placed on the molecule B, the critical temperature is minimized. This results shows that their conductivity strongly depends on an overlap of mainly π orbitals between A and B molecules. Indeed, the TTF-TCNQ complex, which is one of the organic metals at room temperature, has large overlap between donor and acceptor molecules. The structure of quinhydrone at room temperature and atmospheric pressure , however, has less overlap than the TTF-TCNQ. Nakasuji et al. have synthesized derivatives of the quinhydrone whose structure has large overlap. They may exhibit metallic conductivity if the PET state is possible to realize under high pressure. From the results, I conclude that the model (i) exhibits the insulator and the model (ii) exhibits the SDW insulator at low temperature.

From the molecular orbital, these systems have no ionic character rather than neutral character. From these results, I found that the quinhydrone crystal is possible to be mainly (a) and (d) states. However, comparing the averaged total energy of model (i) with that of (ii), the state (a) is more stable than the state (d). If external fields, say pressure, electromagnetic field, and etc., are applied in order to stabilize the state (d), the quinhydrone crystal may exhibit the SDW insulator. Moreover, when the system undergoes to the metastable state of state (d), i.e. $\Delta x = 0.0$, the crystal may exhibits metallic character at room temperature.

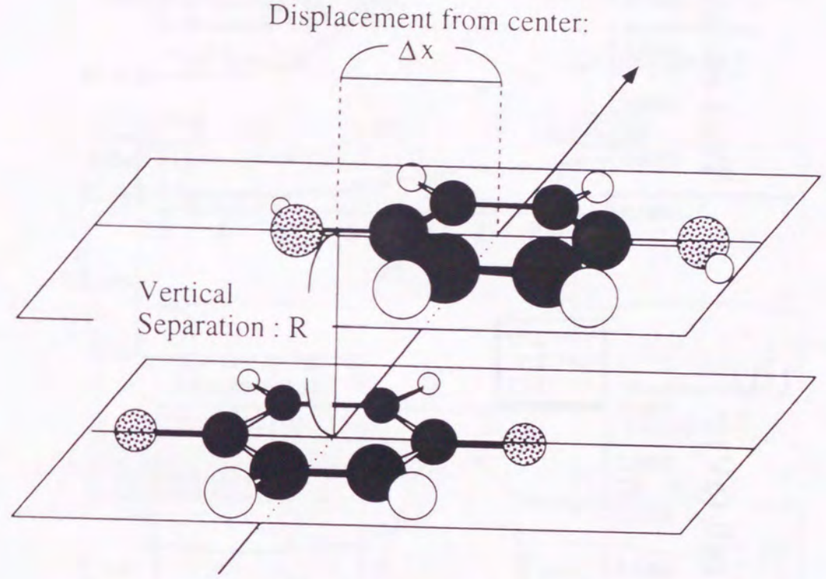

Figure 3.1: A model of a unit cell of the pseudo one-dimensional system

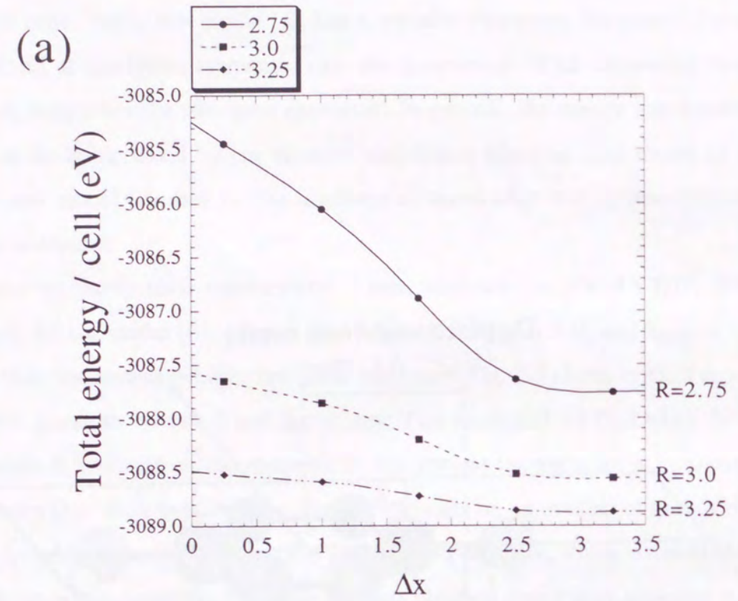

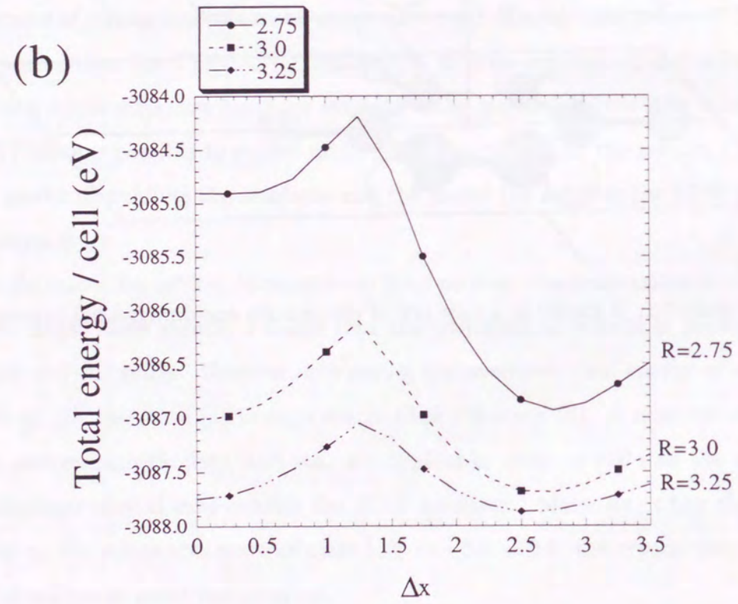

Figure 3.2: Averaged energy of the system (eV): (a) model (i) and (b) model (ii).

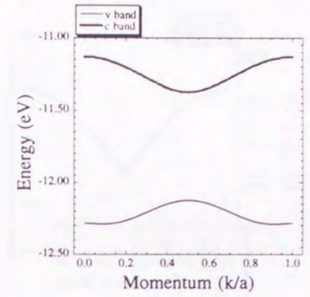

(a) Δx=0.0

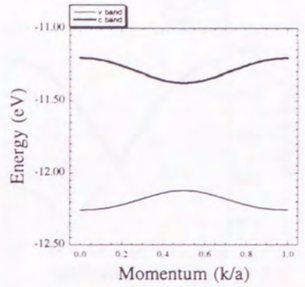

(b) Δx=0.5

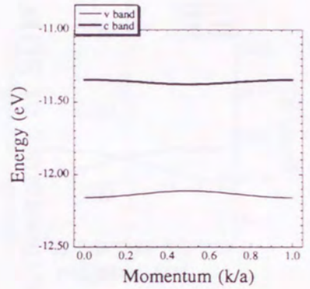

(c) Δx=1.0

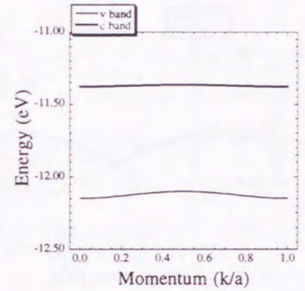

(d) Δx=1.5

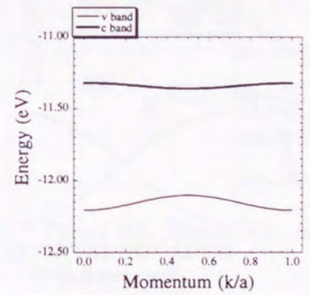

(e) Δx=2.0

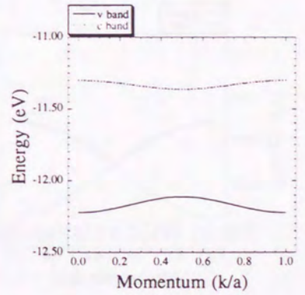

(f) Δx=2.25

Figure 3.3: HOMO and LUMO energy band of model (i) as a functional of Δx at $R =$ 3.25Å. (a) 0.0, (b) 0.5, (c) 1.0, (d) 1.5, (e) 2.0, (f) 2.25 Å.

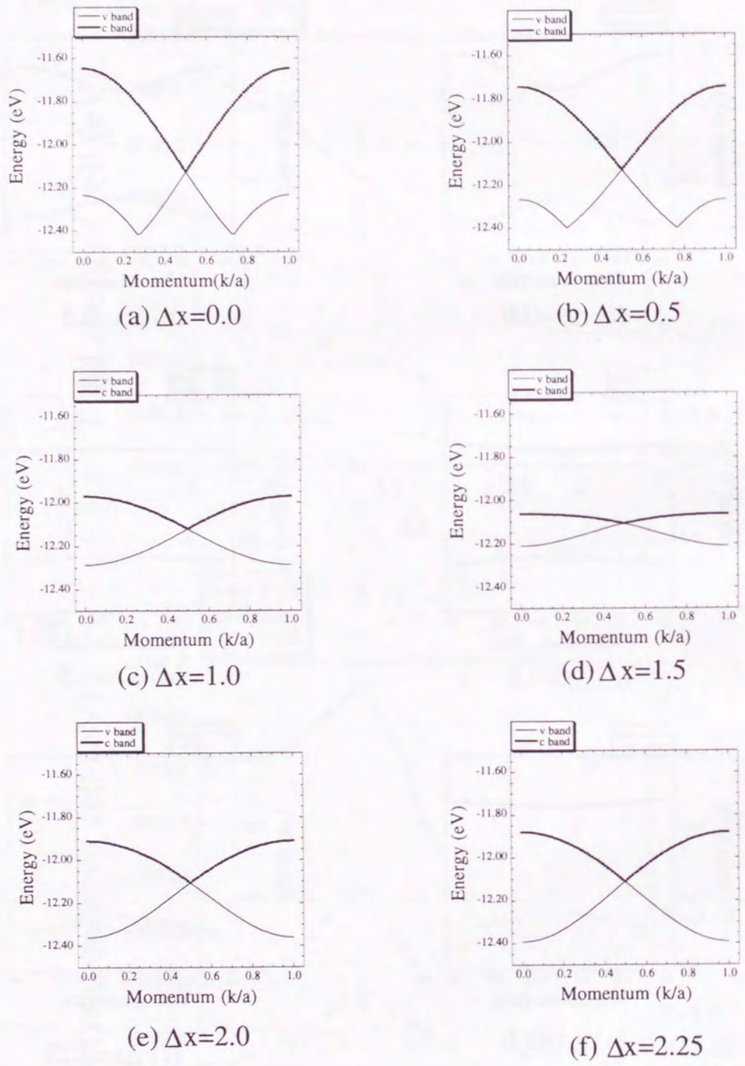

Figure 3.4: HOMO and LUMO energy band of model (ii) as a functional of Δx at $R = 3.25$Å. (a) 0.0, (b) 0.5, (c) 1.0, (d) 1.5, (e) 2.0, (f) 2.25 Å.

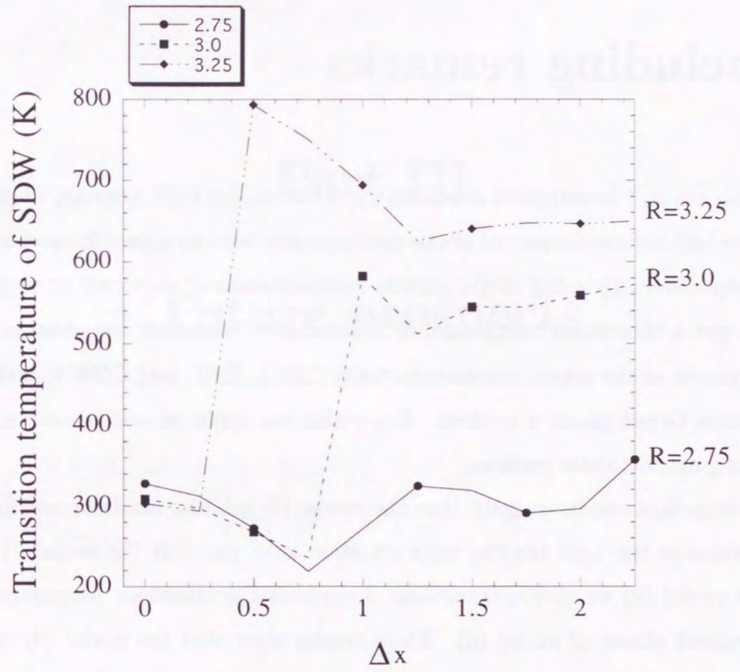

Figure 3.5: Transition temperature from metal to SDW phase.

Chapter 4

Concluding remarks

In this study, I investigated conductivity of two model PET systems, which consist of quinone and hydroquinone and of two semiquinones forming a pseudo one-dimensional chain, respectively, by using single particle representation of electronic structure calculation. I give a theoretical background of calculation of transition temperature of singly ordered phases as the singlet superconductivity (SSC), SDW, and CDW in terms of the temperature Green function method. Especially, we apply an approximation method known as g-model to this problem.

The numerical results suggest that the model (i) exhibits insulator and model (ii) does metallic at the tight binding approximation level and that the model (i) is stable than the model (ii) for all configurations. I calculate the transition temperature of the singly ordered phases of model (ii). These results show that the model (ii) is possible to become the SDW insulator at low temperature and dose not exhibit other phases, CDW and SSC, at any temperature. Moreover, the transition temperature of the SDW becomes lower when the overlap between the donor and acceptor molecules is larger. I suggested a possible mechanism of appearing of the organic metal at room temperature in relation to the PET reaction and applied field. Results of the transition temperature presented here are, however, qualitative rather than quantitative. Although the ab initio treatment and extension to two- and three- dimensional crystals are essential to obtain more quantitative results, it takes vast computational costs and long cpu time. To overcome these difficulties is future problem.

Part III

Future prospects

Chapter 1

Introduction

Here I discuss future problems concerning with a calculation scheme of NBO-DFT and the application to PET systems. I first show the manner of the extension to the quantum dynamics by using real space grid (RSG) method. I next give a short comment about treatment with electronic and nuclear excited states. The excited state DFT is recent topics and many works have been proposed. The time dependent and excited state extension of the NBO-DFT formalism should be very exciting in that from a viewpoint of chemical reactions. Finally, I comment on the thermo filed dynamics, which may mediate between micro and macroscopic phenomena, i.e. quantum and classical phenomena. I also discuss strategy of calculating biological systems in relation to present approaches.

Chapter 2

Application to quantum dynamics

For dynamic cases, molecular dynamics based upon the DFT, which is initiated by Car and Parrinello in 1985 [61], is current topics in the molecular physics. In this method, nuclei are treated as classical particle. However, it is difficult for the method to describe the light mass nuclei such as proton and muon. Nagao have presented the molecular wave packet (MWP) method to investigate the isotope effect on the (hyper) polarizability of one dimensional hydrogen molecule and its isotopomers [62] based upon NBO view point. It is, however, actually trouble to extend these methods into three- dimensional many particle systems, because the method is computationally demanding. In order to reduce the computational efforts, it is necessary to introduce an approximation as possible as retaining accuracy.

I mention here a detail of a real time calculation scheme by means of the RSG, which is an extension of my previous work [26]. I use the fat Fourier transform (FFT) method and local spin density approximation through this section for a first approximation. A discretized one-particle wavefunction is expressed as

$$\phi_i^\sigma(\boldsymbol{r}) = \sum_{l=-N}^{N_s} \sum_{m=-N_s}^{N_s} \sum_{n=-N_s}^{N_s} C_{i,lmn}^\sigma \phi_i^\sigma(x_l, y_m, z_n) \,, \tag{2.1}$$

Although summations are counted over infinite in principle, N_s is restricted to be finite number in actual calculations. I assume that this wavefunction obeys the KS equation. I adopt the higher order expansions for the kinetic operator in Eq.(2.1) by using a uniform

grid. Laplacian operator $\Delta_r \phi_e(x_i, y_j, z_k)$ is approximated as

$$\begin{aligned} \Delta_r \phi_i^\sigma(x_l, y_m, z_n) &= \sum_{n_x=-N_h}^{N_h} C_{n_x} \phi_i^\sigma(x_l + n_x h, y_m, z_n) \\ &+ \sum_{n_y=-N_h}^{N_h} C_{n_y} \phi_i^\sigma(x_l, y_m + n_y h, z_n) \\ &+ \sum_{n_z=-N_h}^{N_h} C_{n_z} \phi_i^\sigma(x_l, y_m, z_n + n_z h) \,, \end{aligned} \tag{2.2}$$

where h is a grid spacing, C_i are constants in the differential method and N_h is a positive integer describing accuracy of this approximation. The accuracy is ordered as $O(h^{2N_h+2})$. The nuclear kinetic terms are also represented in analogical forms. Other approximations for the kinetic operator are referred in [64] and [68]. For isolated systems, I can yield V_H by the FFT in forcing the supercell periodicity, which is commonly used in the calculations of the band structures. Fourier form of the classical Coulomb potential is given by

$$V_H(\boldsymbol{K}) = \sum_{lmn}{}' \frac{4\pi}{|K_l^2 + K_m^2 + K_n^2|} n_t(K_l, K_m, K_n) \,, \tag{2.3}$$

where $n_t(K)$ is fourier form of generalized density defined as

$$n_t(\boldsymbol{r}) = \sum_\sigma n_e^\sigma(\boldsymbol{r}) + \sum_{\alpha I} Z_\alpha n_\alpha^I(\boldsymbol{r}) \,. \tag{2.4}$$

Other treatments to obtain the V_H are the multigrid method solving the Poisson equation [65],[68] and the direct summation method [63]. The exchange-correlation potentials, which depend on the spins of particles, consist of the three parts, which are the exchange part, the correlation with identical particles, and correlation with other particles. The exchange-correlation potential in Eq.(2.18) can be represented as

$$v_{xc}^\sigma[\{n_e^\sigma\}, \{n_\alpha^I\}] = v_{ex}^\sigma + v_c^\sigma + v_{en}^\sigma \,, \tag{2.5}$$

$$V_{xc}^{\alpha I}[\{n_e^\sigma\}, \{n_\alpha^I\}] = V_{ex}^{\alpha I} + V_c^{\alpha I} + V_{en}^{\alpha I} \,, \tag{2.6}$$

Because practical forms of the exchange-correlation potentials are *not* known yet, then I consider a *bold* approximation for the potentials. With these kinetic operators in Eq.(2.2) and the local spin density approximation (LSD), I can construct an one-particle CKSE

over the grid as

$$\begin{aligned}
\hat{F}_e^\sigma \phi_i^\sigma(x_l, y_m, z_n) &= \left[-\frac{1}{2}\Delta_r + V_H(x_l, y_m, z_n) + v_{xc}^\sigma(x_l, y_m, z_n)\right] \phi_i^\sigma(x_l, y_m, z_n) \\
&= \epsilon_i^\sigma \phi_i^\sigma(x_l, y_m, z_n) \,, \\
\hat{F}_\alpha^{I_\alpha} \chi_i^{I_\alpha}(X_l, Y_m, Z_n) &= \left[-\frac{1}{2M_\alpha}\Delta_R - Z_\alpha V_H(X_l, Y_m, Z_n) + \hat{V}_\alpha^{I_\alpha}(X_l, Y_m, Z_n)\right] \\
&\quad \times \chi_i^{I_\alpha}(X_l, Y_m, Z_n) \\
&= E_i^{I_\alpha} \chi_i^{I_\alpha}(X_i, Y_j, Z_k) \,, \qquad (2.7)
\end{aligned}$$

I can obtain the ground state by using the reduction technique [62], which is available from the Taylor expansion of imaginary time evolution operator,

$$\begin{aligned}
\phi_i^\sigma(\tau + d\tau) &= e^{-\hat{F}_e^\sigma(\tau) d\tau} \phi_i^\sigma(\tau) \\
&\approx N_i \left(1 - d\tau \hat{F}_e^\sigma(\tau)\right) \phi_i^\sigma(\tau) + O(d\tau^2) \,, \\
\chi_i^{I_\alpha}(\tau + d\tau) &= e^{-\hat{F}_\alpha^\sigma(\tau) d\tau} \chi_i^{I_\alpha}(\tau) \\
&\approx N_i' \left(1 - d\tau \hat{F}_\alpha^\sigma(\tau)\right) \chi_i^{I_\alpha}(\tau) + O(d\tau^2) \,, \qquad (2.8)
\end{aligned}$$

where N_i and N_i' mean the normalization constant, $\hat{F}_e^\sigma(\tau)$ and $\hat{F}_\alpha^{I_\alpha}(\tau)$ are generated by means of the set of wavefunction $\{\phi_e^\sigma(\tau), \chi_\alpha^{I_\alpha}(\tau)\}$ at time τ. I can obtain the ground state by successively acting the imaginary time evolution operator on the wave function.

This method can be extended into the real time dynamics. Several procedures to expand the real time evolution operator are proposed and their stability has been investigated [69]. For example, second order differential method and the Lanczos method are often used for wavepacket dynamics. Recently, Suzuki [70] proposed a systematic scheme of decomposition of exponential operators and tested its efficiency. Watanabe applied the decomposition method to the real time dynamics of a hydrogen atom under a magnetic field and calculated the spectra of scattering light [71]. This method can be favorable for the real time dynamics of the NBO-DFT calculation scheme, because the method affords a good stability and high accuracy. However, the resultant information on the excited state is approximate one, because the conventional DFT was formulated for evaluation of the ground-state energy. The DFT for excited states is much important for describing the transition states and chemical reactions even for BO case and is current topics in this

area. In the following section, we consider the excited state DFT and its implementation to the NBO case.

An alternative way of real time dynamics including nuclear quantum effects is path-integral based method, i.e. centroid molecular dynamics method, which was initially proposed by Cao and Voth [72] and enable us to treat with the dynamical properties at finite temperature simultaneously. Many applications are performed by using the method, for example, liquid para-hydrogen and that containing the Li impurity, liquid He, and excess proton in water [73]-[75]. I have proposed an extension of the method using spin variables [76]. Recently, fully quantum molecular dynamics method which combines ab initio Car-Parrinello molecular dynamics with centroid molecular dynamics (AICMD) was reported and its application to excess proton translocation along a model water wire was presented [77]. They observed the blue shift from the classical spectra of O-H-O bond and red shift from the classical spectra of weak hydrogen bond O$\cdots$H-O. These shifts are due to quantum effect of the protons. In this method, nuclear motion is treated as an average motion of centroid of an isomorphic classical polymer. It is difficult to perform the calculation with increasing the system size, because the AICMD requires the ab initio calculation for each configuration of the isomorphic polymer. On the other hand, the NBO-DFT requires less computational costs than the AICMD does and, moreover, the extension of the NBO-DFT at finite temperature by using the temperature Green function method and the causal Green function method can be performed.

Chapter 3

Excited state and other problems

Several extensions of the ground state DFT have been contrived to cope with excited states. They are based either on the Reyleigh-Ritz principle for the lowest eigenstate of each symmetry class [79],[80] or on the variational principle for ensembles [81],[82]. The crucial problems are how to determine the exchange-correlation energy functionals for excited states. Recently, Görling suggested a computational scheme for the treatment of excited states within the DFT and the time dependent Kohn-Sham formalism which is generalization of the DFT perturbation [83]. Gross et al. also derived another time dependent DFT with excited states [84]. Levy and Nagy formulated variational scheme for calculation of excited states [85]. They evaluate inonization energy for several atoms, which show good agreements with experimental values. At next stage, making use of these methods may enable us to treat the time dependent molecular dynamics including both ground and excited states by means of the DFT.

Quite independent of the problems connected with the exchange-correlation energy functionals for the excited states, there are some questions that how to uniquely choose the functionals for both the fermion and boson nuclei and for electron-nuclear coupling. At this stage, I have neglected such effects in Eq.(3.9). Here, I will make some remarks about it briefly. For the fermion nucleus, due to the anti-commutation relation or Hund's rule, the identical nuclear-nuclear exchange-correlation terms may be represented as the same form for the electronic-electronic ones. On the other hand, the boson nuclei are satisfied the commutation relation. For the boson nucleus,the Kohn-Sham equation may

be represented as only one differential equation with a density. The identical exchange-correlation terms may be obtained from imperfect Bose gas model taking all these considerations into account. Electron-Nucleus correlation terms, which are third term in the right hand of Eq.(3.9), and different nuclear-nuclear correlation terms are indispensable for describing the nonadiabatic effects. I can *never* neglect these coupling terms. There are many cases in calculating such terms, for example, a correlation between electron and fermion or boson nucleus, between fermion and boson nuclei. Though the last terms are very small in comparison with the other terms, when one investigations on a deuteron in metallic hydrogen and a mixture system of ^{3}He and ^{4}He, the last terms seem to be very significant. Much progress is exceedingly expected to search them, for example, the generalized gradient approximation [86] method with taking advantage of the scaling low generated by the virial theorem [87].

Recent years, applications of time dependent density functional theory (TDDFT) to molecular systems have been performed in order to obtain the excitation spectra, ionization potentials, (hyper-) polarizability and etc. within the RPA and is with great success in describing not only low-lying excited states but also Rydberg states [88]-[90]. The frequency dependent (hyper-) polarizability by using the TDDFT has been performed by Baerends and co-workers [91] and another formulation by using quasi-energy derivative method is derived by Aiga [92]. The GWA also enable us to calculate these values with approximation levels going beyond the RPA systematically. I should take account the contribution of frequency dependent terms in the GWA, the vertex correction to the polarization function, the dynamical collective motions, and the nonadiabatic correction. In future work, I consider these problems in detail.

Chapter 4

Micro- and macroscopic quantum effects

One can observe many phenomena of nature, which are almost macroscopic, and the macroscopic systems exhibit surprisingly various phases. For example, gases → liquids → crystals ; metal → superconductor; antiferromagnet → ferromagnet, which are characterized by crystalline, superconducting and magnetic orders, respectively. It is natural to expect that macroscopic objects are created in a quantum system and the states of the quanta are influenced by the presence of the macroscopic objects. As one of theoretical methods treating thermal effects, I use the temperature Green function method in present work, which is the one of the most widespread methods in the physics. Moreover, in order to investigate the magnetization of model ring molecules I utilized the ab initio path integral approach [78]. I observed the magnetic field induced spin crossover phenomena in the magnetization at low temperature. However, it is difficult for these methods to describe dependency of the thermal effects and thermal averages on real time, because the temperature is interpreted as imaginary time and one need to use mathematically complicated analytic continuations in order to transform it into the real time representation. Moreover, the temperature Green function method is limited to apply to the thermal equilibrium states. There are many other methods based upon the field theory treating thermal phenomena. For example, method of C^* algebra, the Liouville equation and superoperator method, the path ordered method, and thermo field dynamics (TFD)

[93],[94]. In these methods except the TFD, temperature is introduced as an additional parameter. The TFD can treat with temperature and time simultaneously and can be extended to nonequilibrium cases.

It seems that in biological systems motions of the proton and electron mainly dominate the biological phenomena and play an important role in controlling the systems. These are obvious fact because deuteration of water in the biological systems causes to be lost balance of life. In proteins, DNA, and RNA, there exist many hydrogen-bonded networks. The motions of the proton and electron in the hydrogen bond deeply depend on the system and are not sufficiently understood. The hydrogen bonds not only control structure of the systems but also actively contribute to chemical reactions in the systems. The chemical reactions, which partly happen in microscopic active sites of the systems, change into functionalities of life, which can be observed macroscopically. This problem is one of the important subjects to be solved after the 21st century. In the chemical region, it will be crucial to elucidate a mechanism of functionalities in both a molecule (microscopic) and molecular cluster (mesoscopic) levels. Controlling of the chemical reactions and functionalities in the molecular clusters are also matters of great importance. On that occasion, the chemical reactions and functionalities in the biological systems certainly hold the key to the solution and hints of the above questions. As one of interesting problems, there exists a problem that how can Nature chooses the quantum-mechanical, chemical reactions (microscopic) and classical motions (macroscopic) as mentioned before. There is some doubt whether the biological systems make actively use of the quantum mechanical mechanism, because the motions of the solvent, which prevent and promote the chemical reactions in solutions, are well understood in terms of the classical model and the chemical reactions locally happen. Nevertheless, there exists a model for a brain which is based upon quantum field theory, so-called quantum brain dynamics which is based upon the TFD [95],[96]. In this model, dipole moments of the water molecules collectively move. The brain is active due to the bose condensation of the collective motion in the brain, which occurs through evanescent light. If the proton and electron transfer reactions collectively occurs in the hydrogen-bonding networks, the mechanism also is applicable to the other biological systems and the NBO

treatment of the molecular systems may be aid for the elucidation of a new mechanism. With progress in computational equipment and the density functional method, calculation of whole biological molecules will be performed in the near future. However, the elucidation of the chemical reaction and functionalities and as a result of its controlling are farther in the future. Especially, applications of the density functional theory to excited states are begun in the last five years and many quantum chemists are incredulous of them. The NBO Green function method here I present is also a challenging problem. However, this method provides me to treat with quasiparticles of collective motion of the electrons and nuclei and those of nuclei and other kind of nuclei. These treatments with the TFD may open a possibility for describing new phenomena in the biological systems.

Chapter

Appendices

A Outline of density functional theory for electron

I here outline the density functional theory for the many electron system, which shows that the ground-state energy of an interacting system is a unique functional of the ground-state density, originally introduced by Hohenberg and Kohn [40] and modified by Levy[42]. Next, I derive the Kohn-Sham (KS) equation [41] for the system. For simplicity, I restrict ourselves on treating non-degenerate and spin independent cases. Extensions of different cases are straightforward.

A.1 Hohenberg-Kohn theorem

Here, I briefly show the Hohenberg-Kohn theorem and its proof according to a formulation of Levy's constraint search. This theorem is attractive and enables us to treat many-electron system as non-interacting system with an effective potential. In what follows, it is shown that the ground-state energy of an interacting system is a unique functional of the ground-state density and that the functional has a minimum at the exact ground-state density.

Let us define for the system a particle density function $\rho(\boldsymbol{r})$ as

$$\rho(\boldsymbol{r}) = N \int |\Psi(\{\boldsymbol{r}_i\})|^2 d\tau \,, \tag{A-1}$$

where Ψ is ground-state wavefunction normalized to unity and τ is product of volume element except for $d\boldsymbol{r}_1$. If the system is under the influence of an external field, which is derivable from a local scalar potential $u(\boldsymbol{r}_i)$, there is a term in the Hamiltonian describing this interaction:

$$U = \sum_i^N u(\boldsymbol{r}_i) \,. \tag{A-2}$$

Hohenberg and Kohn originally showed that $u(\boldsymbol{r})$ is a unique functional of $\rho(\boldsymbol{r})$. However, it was pointed out that there is not always $u(\boldsymbol{r})$ for physically reliable density $\rho(\boldsymbol{r})$. In what follows, the Levy's version of density functional theory is shown.

Next consider a functional as

$$F[\rho] = \langle \Psi_{min} | T + V_{ee} | \Psi_{min} \rangle \,, \tag{A-3}$$

where Ψ_{min} is antisymmetrized wavefunction minimizing an expectation value of sum of the kinetic energy T and electron repulsion V_{ee}.

Theorem 1: Variational principle for ground-state energy functional

For N-representable $\rho(\boldsymbol{r})$, an energy functional is defined as

$$E[\rho] = \int d\boldsymbol{r} u(\boldsymbol{r})\rho(\boldsymbol{r}) + F[\rho] \,. \tag{A-4}$$

The ground-state energy E_{GS} is lower bound of $E[\rho]$.

Proof of theorem 1

The ground-state energy is given in terms of ground-state wavefunction Ψ_{GS} as

$$E_{GS} = \langle \Psi_{GS} | T + V + U | \Psi_{GS} \rangle \,, \tag{A-5}$$

where $U = \sum_i u(\boldsymbol{r}_i)$. On the other hand, Eq.(A-4) is rewritten as

$$E[\rho] = \langle \Psi_{min} | T + V + U | \Psi_{min} \rangle \,, \tag{A-6}$$

because of the expression as follows:

$$\int d\boldsymbol{r} u(\boldsymbol{r})\rho(\boldsymbol{r}) = \langle \Psi_{min} | U | \Psi_{min} \rangle \,. \tag{A-7}$$

From Eqs.(A-5) and (A-6) and the variational principle, E_{GS} is lower bound of $E[\rho]$, because they are expectation value of the same Hamiltonian.

Theorem 2: N-representablity for ground-state

The ground-state energy E_{GS} is given as a functional with respect to one-particle density of the ground-state

$$E_{GS} = \int d\boldsymbol{r} u(\boldsymbol{r})\rho_{GS}(\boldsymbol{r}) + F[\rho_{GS}] \,. \tag{A-8}$$

Proof of theorem 2

$\Psi_{min}^{\rho_{GS}}$ is antisymmetrized wavefunction minimizing an expectation value of sum of the kinetic energy T and electron repulsion V_{ee} and gives exact ground-state density ρ_{GS}. Note that $\Psi_{min}^{\rho_{GS}}$ do not always identical with Ψ_{GS}. From theorem 1, E_{GS} is lower bound of $E[\rho]$,

$$\langle \Psi_{GS} | T + V + U | \Psi_{GS} \rangle \leq \langle \Psi_{GS}^{\rho_{GS}} | T + V + U | \Psi_{GS}^{\rho_{GS}} \rangle \,. \tag{A-9}$$

Because both $\Psi_{min}^{\rho_{GS}}$ and Ψ_{GS} give the same density $\rho_G S$, then, it is found to be

$$\langle\Psi_{GS}|U|\Psi_{GS}\rangle = \langle\Psi_{GS}^{\rho_{GS}}|U|\Psi_{GS}^{\rho_{GS}}\rangle \,. \tag{A-10}$$

Equation (A-9) can be rewritten as

$$\langle\Psi_{GS}|T+V|\Psi_{GS}\rangle \leq \langle\Psi_{GS}^{\rho_{GS}}|T+V|\Psi_{GS}^{\rho_{GS}}\rangle \,. \tag{A-11}$$

The right side of this equation coincides with $F[\rho_{GS}]$. From the definition of $F[\rho_{GS}]$, the sign of inequality in Eq.(A-9) is contrary. Therefore, the ground-state energy can be represented by ρ_{GS} and the following expression holds for exact density:

$$E_{GS} = \int d\boldsymbol{r} u(\boldsymbol{r})\rho_{GS}(\boldsymbol{r}) + F[\rho_{GS}] \,. \tag{A-12}$$

A.2 Kohn-Sham equation

Kohn and Sham proposed a good approximation for calculations of the ground-state energy and construction of the ground-state density by more efficient way. Ground-state energy of the many-electron system is given by energy functional as Eq.(A-3). Without any approximation, kinetic energy is represented by means of the orbital as follows:

$$T = \sum_i^N n_i \langle\psi_i| - \frac{\nabla^2}{2}|\psi_i\rangle \,, \tag{A-13}$$

where ψ_i and n_i are natural spin orbital and its occupation number. Pauli's principle imposes $0 \geq n_i \geq 1$ and Hohenberg and Kohn theorem guarantees that T is unique functional of total density ρ defined as

$$\rho(\boldsymbol{r}) = \sum_i^N n_i \sum_s |\psi_i(\boldsymbol{r},s)|^2 \,. \,. \tag{A-14}$$

For interacting systems, it is tractable to calculate the kinetic energy, because there are infinite number of terms in Eq.(A-14). Kohn and Sham introduced a quite different method for evaluating $T[\rho]$, which is separated into a major part that is known and a minor correction, showed that one can construct a theory using simpler formulas as

$$T_s[\rho] = \sum_i^N \langle\psi_i| - \frac{\nabla^2}{2}|\psi_i\rangle \,, \,, \tag{A-15}$$

$$\rho(\boldsymbol{r}) = \sum_i^N \sum_s |\psi_i(\boldsymbol{r},s)|^2 \,. \,. \tag{A-16}$$

Equations (A-15) and (A-16) are the special case of (A-13) and (A-14) having $n_i = 1$ for N orbitals and $n_i = 0$ for the rest orbitals.

One can define an energy functional as

$$F[\rho] = T_s[\rho] + J[\rho] + E_{xc}[\rho] \,, \tag{A-17}$$

where

$$E_{xc}[\rho] = T[\rho] - T_s[\rho] + V_{ee}[\rho] - J[\rho] \,. \tag{A-18}$$

$J[\rho]$ is an energy functional of the classical part of Coulomb interaction and E_{xc} is exchange-correlation energy functional, which contains the deference between T and T_s and non-classical part of V_{ee}. KS effective potential is given by

$$\begin{aligned} v_{eff}(\boldsymbol{r}) &= u(\boldsymbol{r}) + \frac{\delta J[\rho]}{\delta\rho(\boldsymbol{r})} + \frac{\delta E_{xc}[\rho]}{\delta\rho(\boldsymbol{r})} \\ &= u(\boldsymbol{r}) + \int d\boldsymbol{r}' \frac{\rho(\boldsymbol{r}')}{|\boldsymbol{r}-\boldsymbol{r}'|} + v_{xc}(\boldsymbol{r}) \,. \end{aligned} \tag{A-19}$$

Now, the Hohenberg-Kohn variational problem is interpreted in terms of Kohn-Sham orbitals appearing in Eq.(A-16). The energy functional can be rewritten as

$$\begin{aligned} E[\rho] &= T_s[\rho] + J[\rho] + E_{xc}[\rho] + \int d\boldsymbol{r}\rho(\boldsymbol{r})u(\boldsymbol{r}) \\ &= \sum_i^N \int d\boldsymbol{r}\psi_i^*(\boldsymbol{r})(-\frac{\nabla^2}{2})\psi_i(\boldsymbol{r}) + J[\rho] + E_{xc}[\rho] + \int d\boldsymbol{r}\rho(\boldsymbol{r})u(\boldsymbol{r}) \,, \end{aligned} \tag{A-20}$$

and electron density as

$$\rho(\boldsymbol{r}) = \sum_i^N |\psi_i(\boldsymbol{r})|^2 \,. \tag{A-21}$$

Define the functional of N orbitals

$$\Omega[\{\psi_i\}] = E[\rho] - \sum_{i,j}^N \varepsilon_{ij} \int d\boldsymbol{r}\psi_i^*(\boldsymbol{r})\psi_j(\boldsymbol{r}) \,, \tag{A-22}$$

where ε_{ij} is Lagrange multiplier ensuring a normalization constraint

$$\int d\boldsymbol{r}\psi_i^*(\boldsymbol{r})\psi_j(\boldsymbol{r}) = \delta_{ij} \,. \tag{A-23}$$

For $E[\rho]$ to be minimum, it is necessary that

$$\delta\Omega[\{\psi_i\}] = 0 \,, \tag{A-24}$$

which leads to an equation

$$h_{eff}\psi_i = \left[-\frac{1}{2}\nabla^2 + v_{eff}\right]\psi_i = \sum_j^N \varepsilon_{ij}\psi_j \,, \tag{A-25}$$

where v_{eff} is determined through Eq.(A-18). Because h_{eff} is Hermite operator, ε_{ij} can be diagnalized to obtain the KS equation in the canonical form as

$$\left[-\frac{1}{2}\nabla^2 + v_{eff}\right]\psi_i = \varepsilon_i\psi_i \,, \tag{A-26}$$

$$v_{eff}(\boldsymbol{r}) = v(\boldsymbol{r}) + \int d\boldsymbol{r}' \frac{\rho(\boldsymbol{r}')}{|\boldsymbol{r}-\boldsymbol{r}'|} + v_{xc}(\boldsymbol{r}) \,, \tag{A-27}$$

$$\rho(\boldsymbol{r}) = \sum_i^N \sum_s |\psi_{is}(\boldsymbol{r})|^2 \,. \tag{A-28}$$

B Greeen function and field theory

In this appendix, the many-body theory for an electron is presented. To describe a system of N electrons, the second quantized formalism is used. I follow the outline of Fetter and Walecka [33], chapters 3, 7, and 13. The utility of the Green function technique is manifold. For one thing, it has a clear and physical interpretation and enables to study single-particle behavior as well as collective phenomena. Further, as stated before, knowledge of the Green functions of a system enables calculating the expectation value of all one-particle operators in the system. There is also a clear prescription how to calculate G, and from this, various schemes of approximation can be developed. I use atomic units through out this appendix.

B.1 Definition of the Green function for zero temperature

The Hamiltonian for the system is given by

$$\begin{aligned}\hat{H} &= \int d\boldsymbol{x}\hat{\psi}^\dagger(\boldsymbol{x})\left[-\frac{\nabla^2}{2} + u(\boldsymbol{x})\right]\hat{\psi}(\boldsymbol{x}) \\ &\quad + \int d\boldsymbol{x}\hat{\psi}^\dagger(\boldsymbol{x})\hat{\psi}^\dagger(\boldsymbol{x}')v(\boldsymbol{x},\boldsymbol{x}')\hat{\psi}(\boldsymbol{x}')\hat{\psi}(\boldsymbol{x}) \,.\end{aligned} \tag{B-1}$$

where $u(\boldsymbol{x})$ is an external potential and $v(\boldsymbol{x},\boldsymbol{x}')$ is the Coulomb interaction. The field operators satisfy the anti-commutation relations as

$$\begin{aligned}\left[\hat{\psi}(\boldsymbol{x}t)\,,\hat{\psi}^\dagger(\boldsymbol{x}'t')\right]_+ &= \delta(\boldsymbol{x}-\boldsymbol{x}')\delta(t-t') \\ \left[\hat{\psi}(\boldsymbol{x}t)\,,\hat{\psi}(\boldsymbol{x}'t')\right]_+ &= \left[\hat{\psi}^\dagger(\boldsymbol{x}t)\,,\hat{\psi}^\dagger(\boldsymbol{x}'t')\right]_+ = 0 \,.\end{aligned} \tag{B-2}$$

For time independent cases, their time dependence is governed by the Hamiltonian H of the system through the field operators in the Heisenberg picture as:

$$\hat{\psi}^{(\dagger)}(\boldsymbol{x}t) = e^{i\hat{H}t}\hat{\psi}^{(\dagger)}(\boldsymbol{x})e^{-i\hat{H}t} \,. \tag{B-3}$$

This follows from the equation of motion for the field operators as

$$i\frac{\partial\hat{\psi}^{(\dagger)}(\boldsymbol{x}t)}{\partial t} = \left[\hat{\psi}^{(\dagger)}(\boldsymbol{x}t)\,,\hat{H}\right]_+ \,. \tag{B-4}$$

Now, the Green function of the system is defined as

$$iG(1,2) = \frac{\langle N|\mathrm{T}\left[\hat{\psi}(1)\hat{\psi}^{\dagger}(2)\right]|N\rangle}{\langle N|N\rangle} = \begin{cases} \frac{\langle N|\mathrm{T}\left[\hat{\psi}(1)\hat{\psi}^{\dagger}(2)\right]|N\rangle}{\langle N|N\rangle} & (t_1 > t_2) \\ -\frac{\langle N|\mathrm{T}\left[\hat{\psi}^{\dagger}(2)\hat{\psi}(1)\right]|N\rangle}{\langle N|N\rangle} & (t_1 < t_2) \end{cases} , \tag{B-5}$$

where abbreviation for a coordinate and time, i.e., $(1) = \boldsymbol{x}_1 t_1$, is used. In what follows, denominator of Eq. (B-5) is normalized to be unity. T is the time ordering operator and $|N\rangle$ is the Heisenberg ground-state of the interacting N-electron system, obeying the Schrödinger equation

$$\hat{H}|N\rangle = E|N\rangle \, . \tag{B-6}$$

The Dyson equation is derived from Eqs. (B-1) and (B-4),

$$\left[i\frac{\partial}{\partial t_1} + \frac{\nabla_1^2}{2} - u(1)\right] G(1,2) = \delta(1,2) - i\int d(3)v(1,2)G_2(1,3,2,3^+)\delta(t_3 - t_1) \, , \tag{B-7}$$

where the two-particle Green function is

$$G_2(1,2,3,4) = (i)^2\langle N|T[\psi(1)\psi(3)\psi^{\dagger}(4)\psi^{\dagger}(2)]|N\rangle \, , \tag{B-8}$$

and $\delta(1,2) = \delta(\boldsymbol{x}_1 - \boldsymbol{x}_2)\delta(t_1 - t_2)$ and $t_3^+ = \lim_{\eta\to+0}(t_3 + \eta)$ are used. The self-energy Σ is defined through

$$\left[i\frac{\partial}{\partial t_1} + \frac{\nabla_1^2}{2} - u(1)\right] G(1,2) = \delta(1,2) - i\int d(3)\Sigma(1,3)G(3,2) \, . \tag{B-9}$$

The non-interacting Green function G_0 is defined as the solution of the following equation

$$\left[i\frac{\partial}{\partial t_1} + \frac{\nabla_1^2}{2} - u(1)\right] G_0(1,2) = \delta(1,2) \, . \tag{B-10}$$

Combining the Eqs.(B-9) and (B-10), the Dyson equation Eq.(B-7) becomes

$$G(1,2) = G_0(1,2) - \int d(3)d(4)G_0(1,3)\Sigma(3,4)G(4,2) \, . \tag{B-11}$$

Although Eq. (B-5) implies luck of much detailed information about the ground-state, the single-particle Green function still contains the observable properties of great interests as follows: (1) the expectation value of any single-particle operator in the ground-state of the system, (2) the ground-state energy of the system, and (3) the excitation spectrum of the system.

B.2 GW approximation

In 1965 Hedin [36] presented a set of coupled equations the should be solved self-consistently to obtain physical properties of G or Σ. I first give some definitions and here present the coupled equations.

The screened interaction W is defined as

$$W(1,2) = \int d(3)v(1,3)\varepsilon^{-1}(3,2) \, , \tag{B-12}$$

where the inverse dielectric function ε^{-1} is defined through the density-density correlation function, which is an extraction of the two-particle Green function defined in Eq.(B-8). This function describes the linear response of the system to an applied external field. The point of the coupled equations is to expand the properties Σ and G in terms of W rather than v. The irreducible polarization propagator P is defined through

$$\varepsilon(1,2) = \delta(1,2) - \int d(3)P(3,2)v(1,3) \, , \tag{B-13}$$

and the three-point vertex function is

$$\Gamma(1,2;3) = \delta(1,2)\delta(1,3) - \frac{\delta\Sigma(1,2)}{\delta V(3)} \, , \tag{B-14}$$

where V is the total average potential of the system, and $\frac{\delta\Sigma(1,2)}{\delta V(3)}$ is the functional derivative of the self-energy with respect to this total average potential.

Finally a set of coupled equations determining Σ is derived as

$$\Sigma(1,2) = i\int d(3)d(4)W(1^+,3)G(1,4)\Gamma(4,2;3) \, , \tag{B-15}$$

$$W(1,2) = v(1,2) + \int d(3)d(4)W(1,3)P(3,4)v(4,2) \, , \tag{B-16}$$

$$P(1,2) = -i\int d(3)d(4)G(2,3)G(4,2)\Gamma(3,4;1) \, , \tag{B-17}$$

$$\Gamma(1,2;3) = \delta(1,2)\delta(1,3) + \int d(4)d(5)d(6)d(7)\frac{\delta\Sigma(1,2)}{\delta G(4,5)}G(4,6)G(7,5)\Gamma(6,7;3) \, . \tag{B-18}$$

These equations are in principle to be solved iteratively to obtain the self-energy Σ as a functional of G. However, this process becomes computationally too complicated to be

carried out even for the electron gas. This mostly due to the presence of the vertex Γ. As as first approximation, Hedin suggested to keep the vertex fixed as 1. This means that Eqs.(B-15) and (B-17) take the form

$$\Sigma(1,2) = i\int d(3)W(1^+,3)G(1,2)\,, \tag{B-19}$$

$$P(1,2) = -iG(1,2)G(2,1)\,. \tag{B-20}$$

The neglect of vertex is similar to the random phase approximation(RPA), but now interacting Green function is used. This scheme is known as GW approximation, because the self-energy in Eq.(B-19) is a convolution over G and W.

B.3 Definition of temperature Green function

It is obvious that including thermal effects is essential to deal with problems in the solid state physics. The finite temperature (Matsubara) Green function, which enable us to discuss dependency of physical properties such as specific heat on temperature and consequently a critical temperature of phase transitions, is presented. The generalization to finite temperature is obtained by replacing the expectation in the ground-state by an average over some statistical ensemble. I here restrict on the case of the grand canonical ensemble.

The average of an operator O in the grand canonical ensemble is

$$\begin{aligned}\langle O\rangle &= \frac{\mathrm{Tr}\left[e^{-\beta(\hat{H}-\mu\hat{N})}O\right]}{\mathrm{Tr}\left[e^{-\beta(\hat{H}-\mu\hat{N})}\right]} = \mathrm{Tr}\left[e^{\beta(\hat{\Omega}-\hat{H}-\mu\hat{N})}O\right] \\ &= \mathrm{Tr}[\hat{\rho}_G O]\,,\end{aligned} \tag{B-21}$$

where $\hat{\Omega}$, $\hat{H}$, μ, and $\hat{N}$ denote a free energy, a Hamiltonian, chemical potential, and a number of particle of a given system, respectively, $\hat{\rho}_G$ is the statistical operator, and the short-handed notation $\beta = 1/k_BT$ is used. The trace (Tr) goes over a complete set of states in which the number of particles is unrestricted. The Heisenberg operator is introduced in terms of grand canonical Hamiltonian $\hat{K} = (\hat{H} - \mu\hat{N})$ as

$$\hat{\psi}^{(\dagger)}(\boldsymbol{x}\tau) = e^{\hat{K}^{(\dagger)}\tau}\hat{\psi}(\boldsymbol{x})e^{-\hat{K}\tau}\,, \tag{B-22}$$

where τ denotes imaginary time, $i\tau = t$. Thus, the temperature Green function is defined by

$$G(1,2) \equiv -\langle\hat{\rho}_G \mathrm{T}_\tau[\psi(1)\psi(2)^\dagger]\rangle\,, \tag{B-23}$$

where the abbreviation of coordinate and (imaginary-) time is again used.

B.4 Bardeen-Cooper-Schrieffer theory for superconductivity

The theoretical explanation of the superconductivity was given by Bardeen, Cooper, and Schrieffer in 1957 and is known as the BSC theory. According to the theory, an electron moving through an elastic lattice creates a distortion of lattice as a result of the Coulomb interaction between ions and the electron. This distortion causes an attractive force between two electrons forming the Cooper pair. A mechanism of the superconductivity is considered as a bose condensation of the Cooper pair. I here summarize a temperature Green function approach for superconducting systems originally proposed by Gor'kov based upon the generalized Hartree-Fock approximation.

For a model of singlet superconductivity, the theory starts from the following model effective grand canonical Hamiltonian for electron gas in a magnetic field

$$\begin{aligned}\hat{K}_{eff} &= \hat{K}_0 + \hat{V}_{eff} \\ &= \int d(1)\hat{\psi}^\dagger_\alpha(1)\left\{\frac{1}{2m}\left[-i\nabla_1 + \boldsymbol{A}(1)\right]^2 - \mu\right\}\hat{\psi}_\alpha(1) \\ &- g\int d(1)\left\{\langle\hat{\psi}^\dagger_\uparrow(1)\hat{\psi}^\dagger_\downarrow(1)\rangle\hat{\psi}_\downarrow(1)\hat{\psi}_\uparrow(1) + \langle\hat{\psi}_\downarrow(1)\hat{\psi}_\uparrow(1)\rangle\hat{\psi}^\dagger_\uparrow(1)\hat{\psi}^\dagger_\downarrow(1)\right\}\,,\end{aligned} \tag{B-24}$$

where $\boldsymbol{A}(1)$ is vector potential and neglected hereafter for simplicity and I use a unit of $(\hbar = e = c = 1)$.

Three different Green functions are defined as follows:

$$G(1,2) = -\langle\mathrm{T}_\tau[\hat{\psi}_\uparrow(1)\hat{\psi}^\dagger_\uparrow(2)]\rangle\,, \tag{B-25}$$

$$F(1,2) = -\langle\mathrm{T}_\tau[\hat{\psi}_\uparrow(1)\hat{\psi}_\downarrow(2)]\rangle\,, \tag{B-26}$$

$$F^\dagger(1,2) = -\langle\mathrm{T}_\tau[\hat{\psi}^\dagger_\downarrow(1)\hat{\psi}^\dagger_\uparrow(2)]\rangle\,. \tag{B-27}$$

The equation of motions for these Green functions are given by

$$\begin{pmatrix} \left[-\frac{\partial}{\partial\tau}-\frac{\nabla_1^2}{2m}+\mu\right]-\delta(1,2) & 0 & \Delta(1) \\ \Delta(1) & \left[-\frac{\partial}{\partial\tau}-\frac{\nabla_1^2}{2m}+\mu\right] & 0 \\ \Delta(1)^* & 0 & \left[\frac{\partial}{\partial\tau}-\frac{\nabla_1^2}{2m}+\mu\right] \end{pmatrix} \times \begin{pmatrix} G(1,2) \\ F(1,2) \\ F^\dagger(1,2) \end{pmatrix} = 0\,, \tag{B-28}$$

with

$$\Delta(1) \equiv gF(1^+;1) = -g\langle\hat{\psi}_\uparrow(1)\hat{\psi}_\downarrow(1)\rangle = g\langle\hat{\psi}_\downarrow(1)\hat{\psi}_\uparrow(1)\rangle\,. \tag{B-29}$$

These equations should be solved iteratively.

In almost cases of interest, the Hamiltonian is time independent and the corresponding Green functions depend only on the difference of time. Moreover, if the system is translationally invariant, it is useful to introduce a Fourier representation,

$$G(1,2) = \frac{1}{\beta}\sum_n e^{-i\omega_n(\tau_1-\tau_2)}\int d\boldsymbol{k}e^{i\boldsymbol{k}\cdot(\boldsymbol{r}_1-\boldsymbol{r}_2)}G(\boldsymbol{k},\omega_n)\,. \tag{B-30}$$

The same relation folds for F and $F^\dagger$. Pair of algebraic equations are obtained as

$$\begin{aligned} (i\omega_n-\xi_k)G(\boldsymbol{k},\omega_n)+\Delta F^\dagger(\boldsymbol{k},\omega_n) &= 0 \\ (-i\omega_n-\xi_k)F^\dagger(\boldsymbol{k},\omega_n)-\Delta^* G^\dagger(\boldsymbol{k},\omega_n) &= 0\,, \end{aligned} \tag{B-31}$$

where $\xi_k \equiv k^2/2m-\mu$. These equations are readily solved to give

$$G(\boldsymbol{k},\omega_n) = \frac{-(i\omega_n+\xi_k)}{\omega_n^2+\xi_k^2+|\Delta|^2}\,, \tag{B-32}$$

$$F^\dagger(\boldsymbol{k},\omega_n) = \frac{-\Delta^*}{\omega_n^2+\xi_k^2+|\Delta|^2}\,. \tag{B-33}$$

In the absence of an applied field, the parameter Δ may be taken as real with no loss of generality, thereby ensuring $F^\dagger(\boldsymbol{k},\omega_n) = F(\boldsymbol{k},\omega_n)$.

A self-consistent equation for Δ is then given

$$\Delta = \frac{g}{\beta}\sum_n\int\frac{d\boldsymbol{k}}{(2\pi)^3}\frac{\Delta}{(\omega_n)^2+\xi_k^2+\Delta^2}\,. \tag{B-34}$$

Canceling the common factor Δ and using a cut off energy in performing above integral, I obtain

$$1 = gN(0)\int_0^{\omega_D}\frac{d\xi}{(\xi^2+\Delta^2)^{1/2}}\tanh\frac{(\xi^2+\Delta^2)^{1/2}}{2k_BT}\,, \tag{B-35}$$

where $N(0) = mk_F/2\pi^2$ is the density of states in the present model. In a limit of $T\to T_c$, the gap vanishes identically and critical temperature T_c can be evaluated as

$$k_BT_c = \frac{2e^\gamma}{\pi}\omega_De^{-1/N(0)g} \approx 1.13\omega_De^{-1/N(0)g}\,. \tag{B-36}$$

Bibliography

1) P. C. E. Stamp, Nature **383**, 125 (1996).

2) L. Thomas et al., Nature **383**, 145 (1996).

3) B. Black, G. Mager, and A. Pines, Chem. Phys. Lett. **201** 550(1993).

4) M. Prager and A. Heidemann, Chem. Rev. **97**, 2933(1997).

5) F. Fillaux, C. J. Carlile, and G. J. Kearley, Phys. Rev. B **44**, 12280(1990).

6) A. Heidemann, H. Freidrich, E. Günther, and W. H"ausler, Z. Phys. B **76**, 335(1989).

7) S. Szymańsky, J. Chem. Phys. **104**, 8216(1996).

8) P. Schiebel, G. J. Kearley, and M. Johnson, J. Chem. Phys. **108**, 2375(1998).

9) P. Schiebel, R. J. Papoular, W. Paulus, H. Zimmermann, A. Detken, U. Haeberlen, and W. Prandl, Phys. Rev. Lett. **83**, 975(1999).

10) D. Hadzi (Ed.) *Theoretical treatment of hydrogen bonding* (John Willey & Sons Inc., Newyork, 1997) and reference therein.

11) M. Prager and A. Heidemann (Eds.), "Rotational Tunneling and Neutron Spectroscopy: A Compilation " (Julich, Germany and ILL, Grenoble, France, 1995).

12) Y. Tominaga and M. Tokunaga, J. Cry. Soc. Jpn **40**, 26(1998) (in Japanese).

13) S. Takeda, F. Kondoh, N. Nakamura and K. Yamaguchi, Physica **B226**, 157(1996).

14) N. Shida, P. F. Barbara and J. Almlöf, J. Chem. Phys. **94**, 3633(1991).

15) M.Born and R.Oppenheimer, Ann. Phys. **84**, 457(1927).

16) E.W.Kaiser, J. Mol. Spectrosc. **13**, 1403 (1988).

17) R. G. Woolley, Adv. Phys. **25**, 27(1976).

18) H. Essén, Int. J. Quantum Chem. **12**, 721(1977).

19) I. L. Thomas, Phys. Rev., **185**,90(1969): I. L. Thomas, Phys. Rev. **A2**, **72**, 728, 1675 (1970); I. L. Thomas and H. W. Joy, ibid **A2**, 1200(1970); I. L. Thomas, ibid **A3**, 565(1971); I. L. Thomas, ibid **A4**, 457(1971); and I.L.Thomas, ibid **A5**, 1104(1972)

20) B. A. Pettit, Chem. Phys. Lett. **130**, 399 (1986). H. J. Monkhorst, Phys. Rev. **A36** 1544(1987).

21) J. F. Capitani, R. F. Nalewajski and R. G. Parr, J. Chem. Phys. **76**, 568(1982).

22) E. S. Kryachko, E. V. Ludena and V. Mujica, Int. J. Quantum Chem. **40**, 589(1991).

23) N. Gidopoulos, Phys. Rev. **A57**, 2146(1998).

24) H. Nagao, K. Kodama, Y. Shigeta, H. Kawabe, K.Nishikawa, M. Nakano and K. Yamaguchi, Int. J. Quantum Chem. **60**, 45(1996).

25) Y. Shigeta, K. Ozaki, K. Kodama, H. Kawabe, H. Nagao and K. Nishikawa, Int. J. Quantum Chem. **69**, 629(1998).

26) Y. Shigeta, H. Takahashi, S. Yamanaka, M. Mitani, H. Nagao and K. Yamaguchi, Int. J. Quantum Chem. **70**, 659(1998).

27) Y. Shigeta, H. Nagao, K. Nishikawa and K. Yamaguchi, Int. J. Quantum Chem. **75**, 875(1999).

28) Y. Shigeta, H. Nagao, K. Nishikawa and K. Yamaguchi, J. Chem. Phys. **111**, 6171(1999).

29) Y. Shigeta, H. Nagao and K. Nishikawa, K. Yamaguchi, J. Chem. Phys. submitted.

30) L. Lathouwers, P. Van Leuven and M.Bouten, Chem. Phys.Lett. **52**, 439(1977); L. Lathouwers, Phys. Rev. **A18**, 2150(1978); E.Deumens, Y.Öhrn, L. Lathouwers, and P. Van Leuven, J Chem Phys. **84**, 3944(1986); and J.Broeckhove, L Lathouwers, and P. Van Leuven, J. Math. Chem. **6**, 207(1991)

31) J. J. Griffin and J. A. Wheeler, Phys. Rev. **108**, 311(1957). D. L. Hill and J. A. Wheeler, Phys. Rev. **89**, 1106(1953).

32) D.M. Blink, A. Weiguni, Nucl. Phys. **A120**, 59(1968).

33) A. L. Fetter and J. D. Waledca, *Quantum Theory of Many Particle System* (McGraw-hill, New York, 1971).

34) L. S. Cederbaum and W. Domcke, Adv. Chem. Phys. **36**, 205(1976).

35) J. Linderberg and Y. Öhrn, *Propagator Method in Quantum Chemistry* (Academic Press, New York, 1973).

36) L. Hedin, Phys. Rev. **139**, A796(1965).

37) L. Hedin and S. Lundqvist, Solid State Phys. **23**, 2(1969).

38) F. Aryasetiawan and O. Gunnarsson, Rep. Prog. Phys. **61**, 237(1998).

39) E. L. Shirley and R. M. Martin, Phys. Rev. **A47**, 15408(1993).

40) P.Hohenberg and W.Khon, Phys.Rev. **136**, B864(1964).

41) W.Kohn and L.J.Sham, Phys.Rev. **140**, A1133(1965).

42) M.Levy, Proc. Natl. Acad. Sci. (USA) **76**, 6062(1979).

43) R.G.Parr and W.Yang, *Density functional Theory of Atoms and Molecules* (Oxford University Press, New York, 1989). and refers therein

44) Katrina S. Werpetinski and M. Cook, Phys. Rev. **A52**, R3397(1995).; Katrina S. Werpetinski and M. Cook, J. Chem. Phys. **106**, 7124(1996).

45) B.I. Dunlap, J. Phys. Chem. **90**, 5524(1986).

46) W.Kolos and L.Wolniewicz, Rev. Mod. Phys. **35**, 473(1963).

47) C. Totsuji and T. Matsubara, J. Phys. Soc. Jpn. **63**, 2760(1994).

48) Y. Noda, H. Kasatani, Y. Watanabe and H. Terauchi, J. Phys. Soc. Jpn. **61**, 1803(1994).

49) T. Matsuo, K. Kohno, A. Inaba, T. Mochida, A. Izuoka and T. Sugawara, J. Chem. Phys. **108**, 9809(1998). ; T. Matsuo, K. Kohno, M. Ohama, T. Mochida, A. Izuoka and T. Sugawara, EuroPhys. Lett. **47**, 36(1999).

50) E. Meggers, M. E. Michel-Beyerle and B. Giese, J. Am. Chem. Soc. **120**, 12950(1998).

51) J. Jortner, M. Bixon, T. Langenbacher and M. E. Michel-Beyerle, Proc. Natl. Acad. Sci. USA **95**, 12759(1998).

52) I. Saito, T. Nakamura, K. Nakatani, Y. Yoshioka, K. Yamaguchi and H. Sugiyama, J. Am. Chem. Soc. **120**, 12686(1998).

53) K. Nakasuji, K. Sugiura, T. Titagawa, J. Toyoda, H Okamoto, K Okaniwa, T Mitani, H Yamamot, I Murata, A, Kawamoto and J Tanaka, J. Am. Chem. Soc. **113**, 1863(1991).

54) T. Mitani, Mol. Cry. Liq. Cry. **171**, 343(1989).

55) M. Kimura, H. Kawabe, K. Nishikawa, and S. Aono, J. Chem. Phys. **85**, 3090, 3097(1986); M. Kimura, H. Kawabe, A. Nakajima, K. Nishikawa, and S. Aono, Bull. Chem. Soc. Jpn. **61**, 4239(1988); M. Kimura, H. Kawabe, K. Nishikawa, and S. Aono, Bull. Chem. Soc. Jpn. **61**, 4245(1988).

56) H. Nagao, M. Mitani, M. Nishino, Y. Shigeta, Y. Yoshioka, and K. Yamaguchi, Int. J. Quantum Chem. **70**, 1075(1998); H. Nagao, M. Mitani, M. Nishino, Y. Shigeta, Y. Yoshioka, and K. Yamaguchi, Int. J. Quantum Chem. **75**, 549(1999); H. Nagao, M. Nishino, Y. Shigeta, Y. Yoshioka, and K. Yamaguchi, J. Chem Phys., submitted.

57) Konsin and Sorkin, Phys. Rev. **B58**, 5795(1998).

58) K. Ohno, Theoret. Chim. Acta. **2**, 219(1964).

59) T. Sakurai, Acta Cryst. **19**, 320(1965), and ibid bf B24, 403(1968).

60) G. A. Landru, YAeHMOP: Yet Another extended Huckel Molecular Orbital Package. YAeHMOP is freely available on the WWW at URL: http://overlap.chem.cornell.edu:8080/yaehmop.html.

61) R.Car and M.Parrinello, Phys.Rev.Lett. **55**, 2471(1985).

62) H.Nagao, K.Kodama, Y.Shigeta, K,Nishikawa, H.Kawabe, and K.Yamaguchi, Int.J.Quant.Chem. **60**, 49(1996); H. Nagao, M. Nakano, S. Yamada, D. Yamaki, I. Shigemoto, S. Kiribayashi, Y. Shigeta, and K. Yamaguchi, Int. J. Quantum Chem. **60**, 60(1996).

63) J.R.Chelikowsky, N.Troullier, and Y.Saad, Phys.Rev.lett. **72**, 1240(1994); J.R.Chelikowsky, N.Troullier, K.Wu and Y.Saad, Phys.Rev.B **50**, 11355(1994); X.Jing, N.Troullier, D.Dean, N.Binggeli, J.R.Chelikowsky, K.Wu, and Y.Saad, ibid **50**, 12234(1994); J.R.Chelikowsky, X.Jing, K.Wu and Y.Saad, ibid **53**, 12071(1996); and X.Jing, J.R.Chelikowsky, and N.Troullier, Solid State Comm. **96**, 231(1996).

64) T.Hoshi, M.Arai, and T.Fujiwara, Phys.Rev.B **52**, R5459(1995).

65) T.L.Beck, Int.J.Quant.Chem. **65**, 477(1997).

66) F.Gygi and G.Galli, Phys.Rev.B **52**, R2229(1995).

67) G.Zumbach, N.A.Modine, and E.Kaxiras, Soild State Comm. **99**, 57(1996).

68) E.L.Briggs, D.J.Sullivan, and J.Bernholc, Phys.Rev.B **52**, R5471(1995) , E.L.Briggs, D.J.Sullivan, and J.Bernholc, ibid **54**, 14362(1996).

69) R. Koslof, J. Phys. Chem **92**, 2087(1988).

70) M. Suzuki, J. Phys. Soc. Jpn. **61**, 3015(1992); Proc. Jpn. Acad. Ser. B **69**, 161(1993).

71) N. Watanabe, M. Tsukada, Abstract of the 5th International Conference of Computational Physics (1999), P1-08.

72) J. Cao and G. A. Voth, J. Chem. Phys. **100**, 5093, 5106(1994), ibid **101**, 6157, 6168, 6184(1994); G. A. Voth, Adv. Chem. Phys. **93**, 135(1996).

73) K. Kinugawa, P. B. Moore, M. L. Klein, J. Chem. Phys., **106**, 1154(1997); ibid **109**, 610(1998).

74) K. Kinugawa, Chem. Phys. Lett. **292**, 454 (1998); K. Kinugawa, H. Nagao, K. Ohta, Chem. Phys. Lett. **307**, 187(1999).

75) M. Pavese, S. Chawla, D. Lu, J. Lobaugh, G. A. Voth, J. Chem. Phys. **107**, 7428(1997).

76) Y. Shigeta, H. Nagao, K. Kinugawa, K. Ohta, K. Yamaguchi, Prog. Theoret. Phys. Suppl. in press.

77) M. Pavese, D. R. Benard, G. A. Voth, Chem. Phys. Lett. **300**, 93(1999).

78) H. Nagao, Y. Shigeta, H. Kawabe, T. Kawakami, K. Nishikawa, K. Yamaguchi, J. Chem. Phys. 107 (1997) 6283; Y. Shigeta, T. Kawakami, H. Nagao, K. Yamaguchi, Synth. Met. 103 (1999) 1989; Y. Shigeta, T. Kawakami, H. Nagao, K. Yamaguchi, Chem. Phys. Lett. **315**, 441(1999).

79) O.Gunnarsson and B.I.Lundqvist, Phys.Rev.B **13**, 4274(1976).

80) U.von Barth, Phys.Rev.A **20**, 1693(1979).

81) A.K.Theophilou, J.Phys.C **12**, 5419(1979); N.Hadjisavvas and A.K.Theophilou, Phys.Rev.A **32**, 720(1985).

82) W.Kohn, Phys.Rev.A **34**, 737(1986); E.K.U.Gross, L.N.Oliveira, and W.Kohn, Phys.Rev.A **37**, 2805, 2809(1988); L.N.Oliveira, E.K.U.Gross, and W.Kohn, Phys.Rev.A **37**, 2821(1988).

83) A.Görling Phys.Rev.A **54**, 3912(1996); ibid **55**, 2630(1997).

84) C.A.Ullrich, U.J.Gossmann, and E.K.U.Gross, Phys.Rev.Lett **73**, 2915(1995).

85) M. Levy, A. Nagy, Phys. Rev. Lett. **83**, 4361(1999).

86) J.P.Perdew, K.Burke, and M.Ernzerhof, Phys. Rev. Lett. **77**, 3865 (1996).

87) P.O.Löwdin, J.Mol.Spect. **3**, 67(1959).

88) C. Jamorski, M. E. Casida, D. R. Salahub, J. Chem. Phys. **104**, 5134(1996); M.E. Casida, C. Jamorski, K.C. Casida, D.R. Salahub, J. Chem. Phys. **108**, 4439(1998).

89) R. Bauernschmitt, R. Ahlrichs, Chem. Phys. Lett. **256**, 454(1996).

90) S. Hirata, M. Head-Gordon, Chem. Phys. Lett. **302**, 375(1999) ; ibid **314**, 291(1999).

91) S. A. J. von Gisbergen, J.G. Snijders, E. J. Baerends, J. Chem. Phys. **109**, 10644(1998); ibid **109**, 10657(1998).

92) F. Aiga, T. Tada, R. Yishimura, J. Chem. Phys. **111**, 2878(1999).

93) H. Umezawa, H. Matsumoto, M. Tachiki, *Thermo Field Dynamics and Condensed States*, (North-Holland, Amsterdam, 1982) and references cited therein.

94) H. Umezawa, *Advanced Field Theory: Micro, Macro, and Thermal Physics*, (the American Institute Physics Press, 1993) and references cited therein.

95) C.I.J.M. Stuart, Y. Takahashi, H. Umezawa, J. Theoret. Biol. **71**, 605(1978).

96) M. Jibu, K. Yasue, *A Physical Pocture of Umezawa's Quantum Brain Dynamics*, in Cybernetics and Systems Research 1992, ed. R. Trapple, World Science Publisher, p. 797.

Publication list

1. "Many-electron-wavepackets method." H. Nagao, M. Nakano, S. Yamada, D. Yamaki, I. Shigemoto, S. Kiribayashi, Y. Shigeta, and K. Yamaguchi, Int. J. Quantum Chem. **60**, 60(1996).

2. "Nonadiabatic treatment of molecular systems by the wavepackets method." H. Nagao, K. Kodama, Y. Shigeta, K. Nishikawa, H. Kawabe, M. Nakano, and K. Yamaguchi, Int. J. Quantum Chem. **60**, 45(1996).

3. "Path integral method by means of generalized coherent states and its numerical approach to molecular systems. I. Ensemble average of total energy." H.Nagao, Y. Shigeta, H. Kawabe, T. Kawakami, K. Nishikawa, and K. Yamaguchi, J. Chem. Phys. **107**, 6283(1997).

4. "Nonadiabatic molecular theory and its application. II. Water molecule." Y. Shigeta, Y. Ozaki, K. Kodama, H. Nagao, H. Kawabe, and K. Nishikawa, Int. J. Quantum Chem. **69**, 629(1998).

5. "Density functional theory without the Born-Oppenheimer approximation and its application." Y. Shigeta, H. Takahashi, S. Yamanaka, M. Mitani, H. Nagao, and K. Yamaguchi, Int. J. Quantum Chem. **70**, 659(1998).

6. "Possibility of charge-mediated superconductors in the intermediate region of metal-insulator transitions." H. Nagao, M. Mitani, M. Nishino, Y. Shigeta, Y. Yoshioka, and K. Yamaguchi, Int. J. Quantum Chem. **70**, 1075(1998).

7. " Quantum phase dynamics of interaction between photon field and magnetic system: effects of magnetic quantum transition." H. Nagao, M. Nakano, Y. Shigeta, and K. Yamaguchi, Opt. Rev. **6**, 227(1999).

8. "Theoretical studies on polarizability of ethylene by path integral method.", Y. Shigeta, H. Nagao, S. Yamada, M. Nakano, K. Ohta and K. Yamaguchi, Synth. Met., **103**, 513(1999).

9. "Theoretical studies of magnetization by ab initio path integral method.", Y. Shigeta, T. Kawakami, H. Nagao, and K. Yamaguchi, Synth. Met. **103**, 1989(1999).

10. " Theoretical studies on anomalous phases in model plane systems of $LiBeH_3$.", H. Nagao, H. Kawabe, Y. Shigeta, M. Nishino, M. Mitani, and K. Yamaguchi, Synth. Met. **103**, 2651(1999).

11. "Density functional theory without the Born-Oppenheimer approximation. II Green function techniques.", Y. Shigeta, H. Nagao, K. Nishikawa, and K. Yamaguchi, Int. J. Quantum Chem. **75**, 875(1999).

12. "Theoretical studies on anomalous phases in molecular systems with external field: Possibility of photo-induced superconductivity." H. Nagao, M. Nishino, M. Mitani, Y. Shigeta, Y. Yoshioka, and K. Yamaguchi, Int. J. Quantum Chem. **75**, 549(1999).

13. "A formulation and numerical approach to molecular systems by the Green function method without the Born-Oppenheimer approximation.", Y. Shigeta, H. Nagao, K. Nishikawa, and K. Yamaguchi, J. Chem. Phys. **111**, 6171-6180(1999).

14. "Theoretical studies of spin level crossing induced by external magnetic field of ring molecule magnet models", Y. Shigeta, T. Kawakami, H. Nagao and K. Yamaguchi, Chem. Phys. Lett. **315**, 441-445(1999).

15. "Quantum Spin Dynamics in Solution toward Quantum Computing", H. Nagao, K. Kinugawa, Y. Shigeta, K. Ohta, and K. Yamaguchi, J. Mol. Liq., in press.

16. "Theoretical studies on the proton and electron transfer (PET) in a pseudo one-dimensional hydrogen bonded network system", Y. Shigeta, Y. Kitagawa, H. Nagao, Y. Yoshioka, J. Toyoda, K. Nakasuji and K. Yamaguchi, J. Mol. Liq.,in press.

17. "Quantum spin dynamics by means of a path integral spin centroid method", Y. Shigeta, K. Kinugawa, H. Nagao, K. Ohta and K. Yamaguchi, Prog. Theor. Phys., in press.